Long-term adaptation to hypoxia provides insight into mechanisms facilitating the switch of *Pseudomonas aeruginosa* to chronic lung infections

Joanna Drabinska[1,2]*, Lucia O'Connor[1,2], Niamh Duggan[1,2], Ciarán J. Carey[1,2], Siobhán McClean[1,2]*

[1]School of Biomolecular and Biomedical Sciences, University College Dublin, Belfield, Dublin, Ireland.

[2]Conway Institute of Biomolecular and Biomedical Science, University College Dublin, Belfield, Dublin, Ireland.

*Corresponding authors

Email: siobhan.mcclean@ucd.ie; joanna.drabinska@ucd.ie

Abstract

Opportunistic bacterial infections are an increasing threat, especially for immunocompromised individuals such as people with cystic fibrosis (CF), driving morbidity and mortality. *Pseudomonas aeruginosa* is a key pathogen that causes chronic lung infections, and has been extensively studied in this context, but the mechanism(s) driving its adaptation towards chronic colonisation in the CF lung is not fully understood.

This work focuses on the adaptations of *P. aeruginosa* to long-term hypoxia, one of the important environmental pressures present in the CF lung, to investigate whether it drives the development of persistence in CF patients. We examined how an early CF strain adapted to 6% oxygen over 28 days using an experimental evolution approach and showed that two distinct *P. aeruginosa* small colony variants (SCVs) emerged, one exclusively in hypoxia-adapted cultures. Importantly, SCVs were more prevalent in hypoxia-adapted cultures than in normoxia-adapted cultures (98% vs <35%). Proteomic analysis revealed significant changes in the abundance of >200 proteins within 28 days, including proteins involved in antibiotic resistance, stress responses, iron acquisition, biofilm formation and proteins previously associated with chronic infection. Importantly the observed stable changes in the proteome were distinct from changes previously reported after short-term exposure to hypoxia. Phenotypic characterisation of adapted cultures supported these findings, showing that hypoxia-adapted cultures developed higher resistance to 8 out of 13 antibiotics tested; increased biofilm (1.8 to 4.1-fold ($p<0.0001$) and decreased pyocyanin production (2.6-fold, $p<0.0001$). All hypoxia-adapted cultures showed decreased siderophore production (2.9 to 3.6-fold, $p<0.02$). Two distinct patterns of adaptation to hypoxic conditions were observed, with the phenotypes of one culture being markedly different from the other two. Overall, we demonstrate that long-term hypoxia exposure contributes to multiple changes in phenotype and proteome that were also observed in *P. aeruginosa* CF lung chronic infection isolates, possibly opening the path to treatment of chronic infections.

Author Summary

Opportunistic antibiotic-resistant bacterial infections are an increasing threat, particularly for immunocompromised individuals such as people with cystic fibrosis (CF). These infections increase disease severity, the number of deaths and healthcare costs. *Pseudomonas aeruginosa* is a major pathogen in this context, causing persistent infections, yet the mechanisms driving its adaptation towards chronic colonisation in the CF lung are not understood.

We investigated the adaptations of *P. aeruginosa* exposed to low oxygen conditions (an important environmental pressure in the CF lung), for 28 days, to examine whether it drives the process of persistence. We found that prolonged exposure to hypoxia induced changes in the pathogen's characteristics, which were distinct from those reported after short term exposure. We observed multiple adaptations in hypoxia adapted cultures, many of which were associated with important signalling networks linked to lifestyle shifts in bacteria and several were also observed in isolates that had adapted to chronic infection. Similar adaptive responses in other opportunistic environmental pathogens suggest that this process of adaptation could be targeted to create universal therapeutic approaches preventing antibiotic overuse and improving patient outcomes.

59 # Introduction

60 Antibiotic-resistant bacterial infections are a growing threat to society. They were associated with
61 nearly five million deaths in 2019 (1), and are expected to cause more than 10 million deaths annually
62 by 2050 (2). Opportunistic pathogens such as *Pseudomonas aeruginosa* play a crucial role in
63 escalating this crisis. While these bacteria typically do not cause infections in healthy people,
64 immunocompromised individuals and people with underlying conditions such as cystic fibrosis (CF)
65 and chronic obstructive pulmonary disease (COPD) or those on ventilator support are at great risk of
66 developing chronic *P. aeruginosa* lung infections (3,4). Moreover, opportunistic pathogens are
67 responsible for the majority of healthcare-associated infections, contributing to increasing morbidity,
68 mortality and costs (5).

69 *P. aeruginosa* is a Gram-negative opportunistic human pathogen, which is a leading cause of
70 nosocomial infections, constituting 11-26% of ventilator-associated pneumonia globally (6). Overall,
71 it causes more than 7% of all health-associated infections and is a major contributor to morbidity and
72 mortality among people with CF (7–9). It has many intrinsic and acquired mechanisms of antibiotic
73 resistance contributing to its spread and persistence (10), and the prolonged antibiotic treatments
74 necessary to manage *P. aeruginosa* chronic infections contribute to the spread of antimicrobial
75 resistance (11,12). Furthermore, the World Health Organisation recognised *P. aeruginosa* as a high
76 priority pathogen in 2024 while the European Centre for Disease Prevention and Control (ECDC)
77 considers it a serious threat (13–16).

78 A key feature of *P. aeruginosa* is its exquisite metabolic flexibility and adaptability to harsh conditions,
79 allowing it to transition from the colonisation of the rhizosphere or hydrosphere to colonising niches
80 within human or animal hosts (4), and establishing persistent infections (17). *P. aeruginosa* isolates
81 from chronic infections generally show different characteristics to those isolated from acute

82 infections, and significantly, chronic infections are extremely difficult to eradicate. Its adaptability is
83 driven by a complex regulatory network involving transcriptional regulators, DNA modifications, non-
84 coding RNAs, quorum sensing, and a range of virulence factors (18–23). Despite this extensive
85 research, the mechanism(s) enabling *P. aeruginosa* to transition from acute to chronic infection
86 remain unclear.

87 *P. aeruginosa*, a facultative anaerobe, thrives under low oxygen/anaerobic conditions using
88 alternative terminal electron acceptors and/or fermentation substrates. Previous studies showed that
89 *P. aeruginosa* preferentially colonizes hypoxic niches within mucus layers of the lung over more
90 oxygenated surfaces (24). *P. aeruginosa* responds to changes in oxygen levels via Anr, which regulates
91 the expression of many of the genes shown to be altered in CF chronic infection (25,26). Studies on
92 another CF-associated pathogen, *Burkholderia cenocepacia* have shown that 40% of genes within a
93 low oxygen activated (Lxa) locus were upregulated in long-term infection isolates from CF patients
94 (27). A subsequent study showed that deletion of single genes from the Lxa or the entire locus
95 resulted in changes in phenotypes crucial for the virulence of this bacterium including host cell
96 attachment, intracellular survival and stress responses (27–29). Given that hypoxia is an important
97 environmental pressure present in the CF lung, we wanted to evaluate the impact of long-term
98 hypoxia exposure on *P. aeruginosa.*

99 To examine the effect of long-term exposure to a low oxygen environment, we developed an
100 experimental evolution approach and demonstrated the impact of long-term exposure to low oxygen
101 conditions on the adaptation of *P. aeruginosa* to chronic lung infections. Our findings provide new
102 insights into the mechanisms that underlie the persistence and virulence of opportunistic bacteria
103 within the host.

104

Results

Design and Optimisation of Experimental Evolution

To investigate the impact of long-term exposure to low oxygen conditions on the adaptation of *P. aeruginosa*, we designed an experimental evolution approach (Fig 1A) exposing the *P. aeruginosa* early infection strain AMT 0023-30 (30,31) to either 6% oxygen or to normoxia (21%) for 28 days. AMT 0023-30 is a well-characterised and sequenced CF paediatric early infection strain that was selected from the international *P. aeruginosa* panel, for which a sequential chronic infection strain is available (AMT 0023-31) (31–33). After considering the ranges of oxygen concentrations that bacteria are exposed to in soil and water, together with the range of hypoxic conditions reported in the CF lung and available literature on physiological tissue hypoxia (24,34,35), we chose 6% oxygen as a low oxygen concentration as it allowed us to observe the response to hypoxia, while not extensively stressing the cells, so that we can distinguish this response from changes associated with anoxia.

Figure 1. Long-term adaptation of *Pseudomonas aeruginosa* to hypoxic conditions. Experimental evolution study design (**A**) and influence of hypoxia on small colony variants emergence (**B to D**). **A.** Workflow of the experimental evolution experiment. **B.** Percentage of SCVs in individual normoxia- and hypoxia adapting cultures over 28 days. **C.** Hypoxia-adapted colony morphotypes observed throughout the long-term adaptation. **D.** Ratios of SCV 1 and SCV 2 in the hypoxia-adapting populations over 28 days. The percentage of the small colony variants in the whole populations was caried out for each flask individually each day of the experiment.

To maintain stable growth over the period of the evolution experiment, daily culture transfer volumes were optimised by evaluating a range of volumes (1-10%) of overnight *P. aeruginosa* cultures transferred into fresh media and analysing their growth patterns (S1 Figure). A 5% volume transfer was chosen as optimal, as it allowed the transfer of the maximum number of bacterial cells without disrupting the growth pattern and resulted in a starting OD_{600} of ~0.1. Examination of growth patterns

129 of the early infection strain revealed a significant difference in the generation times observed during
130 hypoxic and normoxic conditions, with the strain growing 1.8-fold slower under hypoxia (g = 107
131 minutes) compared to normoxia (g = 60 minutes) (S2 Figure). Consequently, during the 28 day
132 adaptation period, the cultures exposed to hypoxia underwent only 377 generations in contrast to
133 677 generations under normoxic conditions.

134 To facilitate further investigation, including phenotyping, proteome analysis, and whole genome
135 sequencing (WGS), three independent flasks were inoculated and incubated under either 6% oxygen
136 or normoxia (21% O_2), and samples were collected every day over 28 days, at the time of culture
137 transfer. The three 28 day, independently adapted populations are referred to as N1, N2, and N3 for
138 replicate normoxia-adapted control populations (NACs) and H1, H2, and H3 for the three replicate
139 hypoxia-adapted cultures (HACs) (Table 1). All the phenotypic characterisation of the individual
140 adapted populations (both HACs and NACs) was performed under normoxic conditions, to ensure the
141 observed changes were stable in the absence of continued hypoxia.

142 **Table 1. List of strains and populations used in this study**

143 144 145

Strain/Population Name		Description	Source
	E	Paediatric early infection cystic fibrosis strain AMT 0023-30	(30)
	L	Paediatric early infection cystic fibrosis strain AMT 0023-31	(30)
NACs	**N1**	28 day normoxia-adapted population, replicate 1	This study
	N2	28 day normoxia-adapted population, replicate 2	This study
	N3	28 day normoxia-adapted population, replicate 3	This study
HACs	**H1**	28 day hypoxia-adapted population, replicate 1	This study
	H2	28 day hypoxia-adapted population, replicate 2	This study
	H3	28 day hypoxia-adapted population, replicate 3	This study

146 Changes in colony morphology and pyocyanin production during 147 adaptation

148 Changes in colony morphology often serve as key indicators of adaptation to the environment. Plating
149 of daily samples from the adapting cultures showed the emergence of small colony variants (SCVs)
150 (Fig 1B) both in NACs and HACs; however, the SCVs appeared earlier during the hypoxia exposure

151 timeframe (Fig 1C). SCVs first appeared on day 2 in the H3 population, and by day 3 in the H1 and H2
152 populations. The SCV abundance peaked at 98% on day 22, with 77% remaining on day 28 in H1.
153 Similarly, the highest proportion of SCVs was reached on day 20 with SCVs comprising 82% of the
154 population, and 80% on the last day of the experimental evolution experiment in flask H2. In contrast
155 in population H3, the SCV abundance was generally lower and more variable, reaching only 50% of
156 the population by day 15, and falling to 1% on day 21. The SCVs appeared much later in normoxic
157 cultures, on days 6, 7 and 8 in flasks N1, N2 and N3 respectively, and only reached a maximum of 25-
158 33% of the population by day 14 (Fig 1C).

159 Two distinct SCV morphologies were observed (Fig 1B and D). The first type, termed SCV 1, was
160 observed both under normoxia and hypoxia, and resembled the morphology most often described as
161 a rugose small colony variant characterised by small size, irregular edges and a heavily wrinkled, dry
162 surface (36). The second type, SCV 2, was slightly bigger than SCV 1 with a similar rough, dry surface;
163 however it was easily distinguished by a more regular edge and shape and importantly, it was
164 exclusive to HACs.

165 Throughout the 28 days of adaptation, we also observed dynamic changes in culture colour (Fig 2A),
166 suggesting changes in pigments, such as pyocyanin. Despite almost no visible change of colour being
167 observed on the day 28 of the experiment (Fig 2A), quantification of pyocyanin production at 28 days
168 revealed that populations H1, H2 and one NAC, N1 produced comparable pyocyanin levels to the late
169 infection strain (AMT 0023-31) (Fig 2B and Fig 2C), suggesting that pyocyanin production is
170 independent of environmental oxygen levels.

171 **Figure 2. Influence of hypoxia on pyocyanin production. A.** Representative photographs of flasks during the
172 28 day experimental evolution study showing changes in pyocyanin production. **B & C.** Quantification of
173 pyocyanin production by individual populations **(B)** and mean values for normoxia- and hypoxia-adapted
174 cultures **(C)** at 28 days, relative to early (E) and late (L) infection strains**.** The data represent the concentration
175 of pyocyanin in 1ml of bacterial culture, calculated as described in the methods. The data represent two

separate experiments performed in normoxic conditions, with at least 3 technical replicates for each strain. Statistically significant differences were determined by ordinary one-way ANOVA test compared to the early infection strain with an uncorrected Fishers LSD test (B.) or Kruskal-Wallis one-way ANOVA test comparing all groups with an uncorrected Dunn's test (C.) are shown (**p< 0.01; ***p<0.001; ****p< 0.0001). E: early infection clinical strain; L: late infection clinical strain; N1, N2, N3: 28-day normoxia-adapted populations; H1, H2, H3: 28-day hypoxia adapted populations.

Influence of hypoxia on the whole proteome

The proteomes of 28 day adapted cultures were analysed to elucidate the overall influence of long-term hypoxia on *P. aeruginosa*. The individual flasks were treated as biological replicates, thus showing the global changes across 3 independent populations. A total of 244 proteins showed significant differences (p≤0.05) in abundance between 28 day HACs and 28 day NACs, of which 205 were altered by 1.5-fold or more (Table 2, S3. Table). The majority of these proteins showed decreased abundance following exposure to hypoxic conditions (n=148; 72.55%), while only 56 proteins (27.45%) showed increased abundance (Table 2). A constructed heatmap showed divergence between the samples from cultures adapted to the same condition (Fig 3A).

Table 2. Proteome comparison of 28 day hypoxia-adapted *P. aeruginosa* populations to normoxia-adapted populations.

Protein groups	Number of proteins*
Total number of identified proteins	1718
Proteins with significantly changed abundance (total)	244
Proteins with significantly changed abundance (by ≥1.5-fold)	205
Proteins unique to hypoxia cultures	5
Proteins unique to normoxia cultures (absent in hypoxia)	16
Proteins with a significantly increased abundance (by ≥1.5-fold) in hypoxia cultures	56
Proteins with a significantly decreased abundance (by ≥1.5-fold) in hypoxia cultures	149

*The proteins with significantly changed abundance were determined using mean LFQ intensities of three independent populations of normoxia and hypoxia-adapted cultures. A fold-change cutoff ≥1.5 was to compare hypoxic and normoxic conditions (T.test p ≤ 0.05)

Functional enrichment

GO biological process functional enrichment analysis identified 35 enriched categories (S4 Table), including those associated with stimulus response, iron-sulphur cluster assembly, and amino acid

203 metabolism. A separate analysis of proteins with increased or decreased abundance in HACs provided
204 further insights into these important processes (Table 3, S2 Table). Overall, 38 GO biological processes
205 were enriched in the increased abundance in hypoxia group (Fig 3B), while 37 processes were
206 enriched in the decreased abundance group (Figure 3B; S2 Table). As expected, hypoxia led to
207 upregulation of processes related to oxygen transport and nitrogen metabolism. Additionally, eight
208 categories relating to nucleotide, nucleoside, ribonucleotide, and ribose phosphate processes were
209 upregulated in hypoxia, together with those associated with gene expression, translation, peptide
210 biosynthesis, and amide biosynthesis. Glutamate biosynthesis and glutamine family amino acid
211 biosynthesis were the only two processes related to amino acid metabolism associated with increased
212 abundance in HACs. In contrast, 18 categories related to amino acid metabolism, including those
213 involving valine, tyrosine, phenylalanine, glutamate, and glutamine, were in the reduced abundance
214 group, suggesting they may be downregulated. Sulphur and iron-sulphur cluster associated processes,
215 chemotaxis, and motility were also associated with proteins that were reduced in abundance.

216 **Figure 3. Whole proteome comparison of long-term hypoxia-adapted and normoxia-adapted *P. aeruginosa.***
217 **A.** Heat map representing expression patterns in adapted populations. The heatmap was generated with the
218 use of Heatmapper (http://heatmapper.ca/) (37). **B.** Dot plot representing functional GoTerm Biological
219 Process enrichment of proteins with increased and decreased abundance in hypoxia. The enrichment analysis
220 and dot plot were prepared using ShinyGo 0.80 (38). Spot size is indicative of the number of proteins involved
221 and the spot colour signifies the relative change in abundance.

222

Table 3. Comparison of GO term biological function enrichment of proteins increased in abundance and decreased in abundance

Increased in abundance	Decreased in abundance
Amino acid metabolism *Glutamate biosynthesis*	Amino acid metabolism *Glutamate metabolism* *L-Phenylalanine metabolism* *Tyrosine catabolism* *Valine metabolism*
Oxygen transport	Iron-sulphur cluster assembley
Nucleotide metabolism *Nucleotide biosynthesis* *Ribonucleotide metabolism*	Response to stimulus *Locomotion* *Chemotaxis*
Protein metabolism	
Peptide biosynthesis	
Amide biosynthesis	
Gene expression	

Blue: functional enrichment of proteins increased in abundance in hypoxia adapted cultures; Orange: functional enrichment of proteins decreased in abundance in hypoxia adapted cultures.

A STRING local network cluster analysis confirmed that the processes associated with proteins that were increased in abundance included translation, protein synthesis, and nucleoside synthesis in hypoxia. It also revealed enrichment in proteins associated with glycolysis and pentose phosphate pathways, including those that were increased and decreased in abundance. Additionally, two mixed categories comprising the *P. aeruginosa* biofilm formation pathway appeared to be upregulated, based on changes in protein abundance. Beyond the downregulation of amino acid and chemotaxis-related pathways identified by GO term enrichment analysis, STRING analysis also highlighted reduced abundance of proteins associated with siderophore production, lipopolysaccharide biosynthesis, fatty acid degradation, quinone biosynthesis, and stress response pathways in hypoxia (S4 Table). KEGG pathway enrichment analysis further highlighted the upregulation of pyrimidine metabolism, ribosome biogenesis, and the alanine, aspartate, and glutamate pathways, alongside the downregulation of siderophore biosynthesis, propanoate metabolism, and amino acid metabolism under hypoxia (S4 Table).

244 **Proteins unique to hypoxia or normoxia**

245 Interestingly, 8.61 % of proteins that showed changes in abundance were either unique to HACs or
246 NACs, as they were present in one condition and were not detected in any of the 3 replicates in the
247 other group. Their consistent presence or absence across all three HACs suggests that their expression
248 is either switched on or off, and consequently, they play critical roles in adapting to low oxygen
249 environments. Only five proteins were unique to HACs (Table 4). These were associated with antibiotic
250 resistance, exopolysaccharide transport, glutamine and arginine metabolism, and cell division. The
251 protein showing the highest abundance among these was PA4456, the ATP-binding component of an
252 ABC transporter. Although other ABC transporter components also showed changes in abundance,
253 they were less dramatic, with fold changes between 1.5 and 6.5-fold. Another protein unique to
254 hypoxia, outer membrane lipoprotein PelC is essential for Pel exopolysaccharide export (39).
255 Glutamate dehydrogenase GdhA, an enzyme in the glutamate biosynthesis pathway and arginine
256 catabolism, was also exclusively detected under hypoxic conditions. Finally, two hypothetical proteins
257 were also unique to HACs: PA3402, involved in transmembrane transport (40), and PA4278, identified
258 as an *E. coli* DedD homolog, a crucial component of the bacterial divisome (41).

259 Proteins that were absent in HACs, and thus potentially redundant in low oxygen conditions, are
260 involved in essential processes such as stress resistance, virulence, regulation (two-component
261 systems), polyamine catabolism, tryptophan biosynthesis, QS, bacterial competition, motility,
262 attachment, biofilm formation and antibiotic resistance (Table 4). Surprisingly, the NarL component
263 of the nitrate-responsive, Anr-regulated system crucial for anaerobic metabolism (42,43), was
264 undetectable in HACs. Proteins important for *P. aeruginosa* virulence were also undetectable in the
265 HACs, including the HptA histidine phosphotransporter, a component of an unorthodox/hybrid two-
266 component system. NqrA NADH dehydrogenase is involved in bacterial competition and protects *P.*
267 *aeruginosa* against autotoxicity (44), while AsnB asparagine synthase and YhfE glutamyl

268 aminopeptidase are both involved in osmotic stress resistance and cell wall stress response (45–48)
269 and the Sbp substrate binding protein is associated with sulphate starvation response and virulence
270 (49,50), were all absent in HACs. Examples of proteins associated with biofilm formation and/or
271 motility that were absent in HACs, include the RidA deaminase (51,52), the PlaB phospholipase B (53)
272 and the PelC exopolysaccharide export associated protein.

273

274 **Table 4. Proteins unique to hypoxia-adapted or normoxia-adapted cultures grouped according to**
275 **function.**

Gene ID[a]	Protein Name	Protein Product Name	H/N[b]	NP[c]	MW[d]	SC[e]
		Stress response				
PA3459	**AsnB**	probable glutamine amidotransferase		8	66.03	17.50
PA3461	**YhfE**	conserved hypothetical protein		6	43.29	21.60
PA0283	**Sbp**	sulfate-binding protein precursor		4	36.43	20.20
		Biofilm/ exopolysaccharide production				
PA3062	**PelC**	PelC		6	18.68	58.10
PA0537	**PA0537**	conserved hypothetical protein		4	22.18	25.20
PA5234	**PA5234**	probable oxidoreductase		4	34.01	14.50
PA2927	**PlaB**	hypothetical protein		4	49.48	5.20
PA3123	**RidA**	RidA subfamily protein		4	34.40	13.52
		Amino acid metabolism				
PA4588	**GdhA**	glutamate dehydrogenase		4	48.85	13.5
PA3713	**SpdH**	spermidine dehydrogenase SpdH		9	68.86	19.5
PA0036	**TrpB**	tryptophan synthase beta chain		6	43.68	18.4
		Transport				
PA4456	**YrbF**	probable ATP-binding component of ABC transporter		5	29.62	26.00
PA3402	**PA3402**	hypothetical protein		5	36.21	21.10
		Other				
PA4278	**PA4278**	hypothetical protein		3	26.08	10.70
PA0991	**HptA**	Histidine phosphotransfer protein HptA		3	38.40	13.29
PA2999	**NqrA**	Na+-translocating NADH: ubiquinone oxidoreductase subunit Nrq1		2	48.08	6.10
PA3879	**NarL**	two-component response regulator NarL		4	24.26	30.10
PA2786	**PA2786**	hypothetical protein		4	17.54	33.50
PA3808	**IscX**	conserved hypothetical protein		4	7.80	62.10
		Function unknown				
PA2530	**PA2530**	hypothetical protein		7	48.96	22.00
PA5136	**PA5136**	hypothetical protein		3	54.32	6.90

276 [a]Gene ID – *P. aeruginosa* PAO1 gene locus ID
277 [b]H/N – Blue: proteins unique to hypoxia-adapted cultures; Red: Proteins absent in hypoxia-adapted cultures
278 [c]NP - Unique peptides: The number of peptide sequences unique to a protein
279 [d]MW - Molecular weight as determined by Q-Exactive LC-MS using *P. aeruginosa* PAO1 reference
280 [e]SC - % sequence covered by matching peptides for the identified protein

281

282 ## Antibiotic resistance of adapted cultures

283 A change in the abundance of 48 proteins associated with antibiotic resistance was observed in HACs
284 (Table 5), with 25 showing increased abundance. Notably, type VI secretion system proteins, and TopA
285 topoisomerase, all previously associated with resistance to various classes of antibiotics, were
286 increased in abundance; however, in contrast, MexA and OprM efflux pump proteins, DNA turnover
287 proteins (e.g. elongation factor G, MutL) and cell envelope biosynthesis proteins showed decreased
288 abundance.

289 **Table 5. Examples of proteins altered by ≥ 1.5-fold in *P. aeruginosa* hypoxia-adapted cultures**
290 **relative to normoxia-adapted cultures.**

Gene ID[a]	Protein Name	Fold Change	Protein Product Name	Function[b]	NP[c]	MW[d]	SC[e]
PA3402	**PA3402**	U	hypothetical protein	Antibiotic res	5	36.21	21.10
PA3062	**PelC**	U	PelC	Biofilm	6	18.68	58.10
PA4456	**YrbF**	U	probable ATP-binding component of ABC transporter	Antibiotic res	5	29.62	26.00
PA2664	**Fhp**	6.52	flavohemoprotein	Stress res	7	43.66	27.50
PA3163	**Cmk**	5.50	cytidylate kinase	Antibiotic res	3	24.64	21.80
PA5346	**SadB**	3.39	SadB	Biofilm, Motility	5	51.43	19.60
PA3559	**PA3559**	3.20	Probable nucleotide sugar dehydrogenase	Biofilm	3	51.80	10.60
PA0091	**VgrG1**	2.60	VgrG1	Antibiotic res	5	72.01	22.90
PA2900	**PA2900**	2.47	probable outer membrane protein precursor	Antibiotic res	5	29.85	30.90
PA4753	**YhbY**	2.46	conserved hypothetical protein	Antibiotic res	9	11.66	88.50
PA5549	**GlmS**	2.34	glucosamine-fructose-6-phosphate aminotransferase	Antibiotic res	30	66.29	49.60
PA0762	**AlgU**	2.19	Sigma factor AlgU	Biofilm, Motility	7	22.20	52.30
PA0083	**TssB1**	2.10	TssB1	Antibiotic res, Biofilm	13	18.79	73.80
PA0084	**TssC1**	2.00	TssC1	Antibiotic res, Biofilm	31	55.77	69.70
PA0141	**Ppk2**	1.97	GDP-polyphosphate phosphotransferase	Biofilm	20	40.79	72.80
PA4131	**PA4131**	1.90	probable iron-sulfur protein	Fe acq.	15	63.99	24.80
PA5117	**TypA**	1.88	regulatory protein TypA	Antibiotic res, Motility	22	66.93	35.70
PA0067	**PrlC**	1.85	oligopeptidase A	Antibiotic res, Motility	35	76.04	40.80
PA1673	**Mrh**	1.82	Microoxic hemerythrin	Biofilm	5	17.85	37.30
PA0998	**PqsC**	1.70	PqsC	Antibiotic res	16	38.24	55.50
PA3011	**TopA**	1.70	DNA topoisomerase I	Antibiotic res, Stress res, Biofilm	37	97.28	51.80
PA3617	**RecA**	1.60	RecA protein	Antibiotic res	12	36.88	36.40
PA4748	**TpiA**	1.59	triosephosphate isomerase	Antibiotic res	10	25.62	44.20
PA3810	**HscA**	1.57	Heat shock protein HscA	Fe acq.	13	66.45	22.60
PA0588	**yeaG**	-1.56	conserved hypothetical protein	Antibiotic res, Motility	55	73.72	67.70
PA4595	**ArtR**	-1.56	ATP-activated Repressor of T3SS regulator	Antibiotic res	39	61.32	61.40
PA5078	**OpgG**	-1.59	OpgG	Stress res, biofilm	14	59.48	34.90
PA2553	**PA2553**	-1.60	probable acyl-CoA thiolase	Antibiotic res	43	41.40	90.90
PA3529	**TsaA**	-1.66	alkylhydroperoxide reductase C	Stress res	28	21.82	84.00
PA4406	**LpxC**	-1.70	UDP-3-O-acyl-N-acetylglucosamine deacetylase	Antibiotic res	17	33.44	54.50
PA3723	**YqjM**	-1.72	probable FMN oxidoreductase	Antibiotic res, Stress res	24	40.32	80.40
PA0758	**PA0758**	-1.74	hypothetical protein	Stress res	10	30.88	47.50
PA2552	**AcdB**	-1.85	probable acyl-CoA dehydrogenase	Antibiotic res, Motility	14	40.91	46.40
PA2532	**Tpx**	-1.90	thiol peroxidase	Antibiotic res, Stress res, Biofilm	18	17.23	99.40
PA2071	**FusA2**	-1.96	elongation factor G	Antibiotic res	31	77.57	70.40

PA4946	**MutL**	-2.08	DNA mismatch repair protein MutL	Antibiotic res	12	69.75	25.60
PA4876	**OsmE**	-2.11	osmotically inducible lipoprotein OsmE	Stress res	7	12.52	41.20
PA1097	**FleQ**	-2.14	Transcriptional regulator FleQ	Biofilm, Motility	23	55.28	58.00
PA5285	**SutA**	-2.17	SutA	Biofilm	12	11.17	93.30
PA0427	**OprM**	-2.20	Major intrinsic multiple antibiotic resistance efflux outer membrane protein OprM precursor	Antibiotic res, Stress res	14	52.60	32.60
PA3017	**PA3017**	-2.32	Universal stress protein	Stress res	11	15.84	84.80
PA2015	**LiuA**	-2.38	putative isovaleryl-CoA dehydrogenase	Antibiotic res	20	42.21	55.80
PA2639	**NuoD**	-2.49	NADH dehydrogenase I chain C,D	Antibiotic res	27	68.32	50.30
PA1041	**PA1041**	-2.55	Probable outer membrane protein precursor	Biofilm	13	21.75	49.50
PA2009	**HmgA**	-2.55	homogentisate 1,2-dioxygenase	Stress res	17	47.84	50.50
PA3922	**PA3922**	-2.55	conserved hypothetical protein	Antibiotic res, Biofilm	17	51.23	54.30
PA0473	**PsfA**	-2.62	probable glutathione S-transferase	Fe acq.	6	28.33	22.90
PA1561	**Aer**	-2.65	Aerotaxis receptor Aer	Motility	18	57.18	45.70
PA5111	**GloA3**	-2.73	lactoylglutathione lyase	Antibiotic res	3	20.21	31.80
PA4290	**PA4290**	-2.92	probable chemotaxis transducer	Antibiotic res, Motility	16	58.40	37.20
PA4515	**PiuC**	-3.04	conserved hypothetical protein	Antibiotic res, Fe acq.	7	25.62	31.00
PA2867	**PA2867**	-3.07	Probable chemotaxis transducer	Motility	8	51.46	34.90
PA1753	**PA1753**	-3.10	conserved hypothetical protein	Antibiotic res, Stress res	4	18.37	33.30
PA4310	**PctB**	-3.13	Chemotactic transducer PctB	Motility	8	68.08	45.80
PA2008	**FahA**	-3.16	fumarylacetoacetase	Antibiotic res	15	46.34	41.20
PA2764	**PA2764**	-3.27	Hypothetical protein	Motility	7	24.52	33.30
PA0887	**AcsA**	-3.28	acetyl-coenzyme A synthetase	Antibiotic res	45	71.76	64.40
PA3795	**PA3795**	-3.50	probable oxidoreductase	Stress res	7	34.80	31.30
PA2920	**PA2920**	-3.57	probable chemotaxis transducer	Stress res, Motility	10	58.32	23.10
PA4221	**FptA**	-3.76	Fe(III)-pyochelin outer membrane receptor precursor	Fe acq.	25	79.99	42.20
PA4738	**YjbJ**	-4.09	conserved hypothetical protein	Stress res	5	7.61	75.40
PA2638	**NuoB**	-4.11	NADH dehydrogenase I chain B	Antibiotic res	9	25.43	36.40
PA0250	**PA0250**	-4.35	conserved hypothetical protein	Stress res	6	15.67	59.00
PA2652	**PA2652**	-4.67	Methyl-accepting chemotaxis protein	Motility	10	60.34	26.60
PA1092	**FliC**	-4.76	Flagellin type B	Bbiofilm, Motility	6	49.24	15.60
PA0425	**MexA**	-4.83	Resistance-Nodulation-Cell Division (RND) multidrug efflux membrane fusion protein MexA precursor	Antibiotic res	19	40.97	48.60
PA4223	**PchH**	-4.88	probable ATP-binding component of ABC transporter	Antibiotic res, Motility	9	61.34	20.70
PA0744	**PA0744**	-4.89	Probable enoyl-CoA hydratase/isomerase	Mot	14	40.59	38.70
PA3938	**TauA**	-5.11	probable periplasmic taurine-binding protein precursor	Antibiotic res, Stress res	9	35.86	50.10
PA3812	**IscA**	-5.34	probable iron-binding protein IscA	Antibiotic res, Fe acq.	4	11.57	51.40
PA3819	**YcfJ**	-5.67	conserved hypothetical protein	Antibiotic res, Stress res	9	18.97	63.20
PA2363	**HsiJ3**	-5.94	HsiJ3	Antibiotic res	5	47.78	19.20
PA4225	**PchF**	-5.98	pyochelin synthetase	Fe acq.	67	197.08	38.50
PA2788	**PA2788**	-6.13	Probable chemotaxis transducer	Motility	14	56.39	36.90
PA4226	**PchE**	-6.46	dihydroaeruginoic acid synthetase	Fe acq.	47	156.42	34.10
PA4224	**PchG**	-7.13	pyochelin biosynthetic protein PchG	Fe acq.	12	37.70	35.50
PA1065	**PA1065**	-7.68	conserved hypothetical protein	Antibiotic res	3	17.99	24.20
PA3441	**SsuF**	-7.71	probable molybdopterin-binding protein	Stress res	3	7.59	47.90
PA4230	**PchB**	-7.77	salicylate biosynthesis protein PchB	Antibiotic res, Fe acq.	12	11.43	62.40
PA2640	**NuoE**	-8.00	NADH dehydrogenase I chain E	Antibiotic res, Mot	6	18.09	60.20
PA2717	**Cpo**	-8.42	chloroperoxidase precursor	Stress res, Biofilm	9	30.44	59.10
PA2033	**ViuB**	-10.88	hypothetical protein	Fe acq.	6	33.65	28.50
PA5131	**Pgm**	-12.57	phosphoglycerate mutase	Antibiotic res	7	55.60	17.70
PA4825	**MgtA**	-17.09	Mg(2+) transport ATPase, P-type 2	Stress res, Fe acq.	41	100.05	32.80
PA4227	**PchR**	-20.62	transcriptional regulator PchR	Fe acq.	3	32.34	14.90
PA0283	**Sbp**	U	sulfate-binding protein precursor	Stress res	4	36.43	20.20
PA0537	**PA0537**	U	Conserved hypothetical protein	Biofilm	4	22.18	25.20
PA2786	**PA2786**	U	hypothetical protein	Antibiotic res	4	17.54	33.50
PA2927	**PlaB**	U	Hypothetical protein	Biofilm	4	49.48	5.20
PA3123	**RidA**	U	RidA subfamily protein	Biofilm, Motility	4	13.52	34.40
PA3459	**AsnB**	U	probable glutamine amidotransferase	Stress res	8	66.03	17.50
PA3461	**YhfE**	U	conserved hypothetical protein	Stress res	6	43.29	21.60
PA3808	**IscX**	U	conserved hypothetical protein	Fe acq.	4	7.80	62.10
			Increased in abundance (fold)		1.5-2	2-5	≥5
			Decreased in abundance (fold)		1.5-2	2-5	≥5

Blue shading represents proteins increased in abundance or unique to hypoxia. Dark blue: ≥5-fold increase in abundance; medium blue: 2- to 5-fold increase in abundance, light blue: 1.5- to 2-fold increase in abundance. Orange shading represents proteins decreased in

293 abundance in hypoxia or absent in hypoxia. Dark orange: ≥5-fold decrease in abundance; medium orange: 2- to 5-fold decrease of
294 abundance; light orange: 1.5- to 2-fold decrease in abundance.
295 [a]Gene ID – *P. aeruginosa* PAO1 gene locus ID.
296 [b]Relevant protein function. Antibiotic res: antibiotic resistance; Stress res: stress resistance; biofilm: Biofilm formation and/or
297 exopolysaccharide production; Fe acq.: iron acquisition and/or homeostasis; Motility: motility.
298 [c]NP - Unique peptides: The number of peptide sequences unique to a protein
299 [d]MW - Molecular weight as determined by Q-Exactive LC-MS using *P. aeruginosa* PAO1 reference (kDa)
300 [e]SC - % sequence covered by matching peptides for the identified protein
301 [f]U – Proteins unique to hypoxia or absent in hypoxia

302 To confirm whether the alterations of proteins associated with antibiotic resistance affect the
303 phenotype of each of the individually adapted cultures, antibiotic susceptibility was examined.
304 Changes in sensitivity to a wide range of antibiotic classes were observed in both HACs and NACs
305 compared to the early infection strain (Fig 4). However, both H1 and H2 populations clearly showed
306 more increases in antibiotic resistance than any other cultures, correlating with the changes in protein
307 abundance. Increased resistance to fluoroquinolones, macrolides, cephalosporins, carbapenems and
308 penicillins was observed in both H1 and H2 cultures, together with decreased resistance to
309 aztreonam. Interestingly, the H3 culture only showed an increased resistance to aztreonam with no
310 change in susceptibility to any other antibiotic tested. All strains were resistant to tetracycline.

311 **Figure 4. Effects of long-term hypoxia adaptation on antibiotic resistance and stress resistance**. **A.** Graphs
312 represent the antibiotic susceptibility of early infection control strain AMT 0023-30, late infection strain, AMT
313 0023-31, and 28-day adapted populations using diffusion discs, tested in normoxic conditions. Bars represent
314 the mean inhibition zone diameter. The data represent three biological replicates and error bars represent the
315 standard deviation. The statistical significance was determined with the nonparametric Kruskal-Wallis test in
316 combination with uncorrected Dunns multiple comparisons test. **B**. Summary of antibiotic resistance to all
317 tested antibiotics. **C.** Determination of stress resistance with droplet assays. Representative pictures of
318 colonies from serial dilutions of each strain plated on agar with the specific stress factor added. The
319 experiments were performed in normoxic conditions at least 3 times for each stress type with the early
320 infection strain as a control. **D.** Table summarising changes in stress sensitivity. ↑ - increased resistance; ↓ -
321 decreased resistance; = no significant difference in resistance; R – no inhibition zone observed. E: early
322 infection clinical strain; L: late infection clinical strain; N1, N2, N3: 28-day normoxia-adapted populations; H1,
323 H2, H3: 28-day hypoxia adapted populations.

324 ## Hypoxia-adapted cultures show changes in stress response

325 Many proteins related to stress responses showed changes in abundance in response to long-term
326 exposure to hypoxia (Table 4), including universal stress proteins (PA3017, PA1753); osmotic stress
327 response associated proteins (OpgG, OsmE, PA2920, PA4738, PA3461, AsnB); oxidative stress
328 response associated proteins (Ftp, TsaA, PA3723, Tpx, PA0250, TauA, OprM, MexA, TopA, Hmg, Cpo);
329 heat-shock stress response associated proteins (TopA, PA0758), sulphate starvation (SsuF, Sbp); cell
330 wall stress/envelope stress response proteins (PA3819, PA3795) and cadmium stress response (MgtA)
331 (Table 5).

332 To examine the impact of these alterations on the phenotype of each of the individual populations,
333 droplet stress plates were prepared to test a range of stresses described as hallmarks of the CF lung
334 environment. No clear pattern of resistance to high temperature, osmotic or acidic stress between
335 the HACs and NACs was observed (Fig 4). Interestingly, increased resistance to oxidative stress was
336 observed in both H1 and H2 cultures and in the N3 culture, which were also the only populations
337 where SCVs had been detected on day 28, and where increased biofilm production and
338 exopolysaccharide production were observed (Fig 4).

339 ## Hypoxia-adapted cultures show increased biofilm formation and
340 ## exopolysaccharide production

341 Typically, anaerobic conditions promote biofilm formation, with greater numbers of live bacteria,
342 increased thickness, and more compact structures (54). In this work, changes in the abundance of 20
343 proteins associated with biofilm and/or exopolysaccharide production were observed in response to
344 exposure to 6% oxygen (Table 5). Nine showed increased abundance or were unique to hypoxia,
345 including the PelC exopolysaccharide export protein, as already mentioned. Others included proteins
346 involved in surface attachment (SadB), exopolysaccharide production (PA3559, AlgU), and type VI

347 secretion system (TssB1, TssC1). Proteins that showed decreased abundance are involved in the
348 switch from a planktonic to a biofilm lifestyle (RidA); biofilm formation and structure, and cell
349 attachment (PlaB, PA1041, SutA, FleQ, OpgG); alginate production (Cpo); flagellin (FliC).

350 To confirm the impact of these proteome changes on biofilm and exopolysaccharide production,
351 these phenotypes were examined in each individual adapted culture (Fig 5A and 5B). Only H1 and H3
352 populations showed a significantly increase in biofilm formation as compared to the early infection
353 patient strain (6.1- and 4.3-fold increases respectively) after 24 h. Significant increases in biofilm
354 production were also observed in the late strain (1.6-fold), H1 (3.9-fold) and H2 (1.4-fold) over the
355 early strain at 48 h, and this trend persisted at 72h (Fig 5A). The increased biofilm production of the
356 H3 population was transient and reverted to AMT 0023-30 early infection strain levels by 48 hours.
357 Congo Red staining revealed darker colonies for H1 and H2 populations which were more wrinkly than
358 in the other strains indicating a higher production of exopolysaccharides (Fig 5B). Interestingly, a
359 similar phenotype was observed in culture N3, again suggesting that this phenotype is not solely
360 dependent on oxygen exposure.

361 **Figure 5. Effects of long-term hypoxia adaptation on biofilm formation, exopolysaccharide production and**
362 **siderophore production. A.** Biofilm formation capability of hypoxia-adapted cultures determined with the
363 crystal violet assay after 24, 48 or 72h of static incubation on a 96-well plate in normoxic conditions. Data
364 represent the mean value of the OD_{590}/OD_{600} ratio from three separate experiments with at least 6 technical
365 replicates for each strain. Statistically significant difference by Kruskal-Wallis one-way ANOVA test compared
366 to the early infection strain (E) with an uncorrected Dunn's test (**p< 0.01; ***p<0.001; ****p< 0.0001). **B.**
367 Exopolysaccharide production by the adapted cultures. The photographs show colonies of different
368 populations of bacteria. The change of colour to a darker shade and a wrinkly colony surface indicate a higher
369 exopolysaccharide production. **C.** Pyochelin synthesis pathway. Pink: proteins decreased in abundance in the
370 proteome of hypoxia-adapted populations. **D.** Siderophore production represented as the mean of
371 siderophore units produced by each colony forming unit, tested in normoxic conditions. Statistically significant
372 differences by ordinary one-way ANOVA test compared to the early infection strain with an uncorrected
373 Fishers LSD test are shown (*p<0.05; **p< 0.01). E: early infection clinical strain; L: late infection clinical strain;
374 N1, N2, N3: 28-day normoxia-adapted populations; H1, H2, H3: 28-day hypoxia adapted populations. E: early

375 infection clinical strain, AMT 0023-30; L: late infection clinical strain, AMT 0023-31; N1, N2, N3: 28-day
376 normoxia-adapted populations; H1, H2, H3: 28-day hypoxia adapted populations.

377 Adaptation to hypoxia affected iron acquisition and homeostasis

378 Proteomic analysis showed changes in the abundance of 14 proteins related to iron homeostasis and
379 acquisition pathways (Table 5). More than half of the proteins in the pyochelin biosynthesis pathway
380 were decreased in abundance by 6-fold or more (PchB, PchE, PchF, PchG) (Fig 5C), and the master
381 regulator of pyochelin production, PchR, was decreased in abundance by over 20-fold. Additionally,
382 the abundance of several iron transport proteins was decreased, including FptA (iron-bound
383 pyochelin receptor), ViuB (siderophore uptake protein), PiuC (Fe(II)-dependent dioxygenase), MgtA
384 (involved in citrate-bound iron transport into the cell), and PsfA (a stress protein involved in iron
385 acquisition). Moreover, the abundance of proteins involved in iron-sulphur cluster biosynthesis was
386 also affected by hypoxia with HscA increased in abundance nearly 1.6-fold, IscA decreased in
387 abundance over 5.3-fold and IscX undetectable in HACs.

388 Differences in iron acquisition and siderophore levels of all individual populations were examined and
389 the results were consistent with the overall proteome analysis, showing a clear decrease in
390 siderophore production in all of the HACs by 2.8- to 3.6-fold ($p<0.05$), but no significant changes in
391 the NACs (Fig 5D). Moreover, a similar change was observed between the early infection strain and
392 late infection strain, with a 4-fold decrease in siderophores ($p<0.01$), highlighting that hypoxia is likely
393 to drive this adaptation at least in part.

394 Adaptation to hypoxia induces changes in motility

395 Sixteen proteins associated with motility showed decreased abundance in the HACs, while only three
396 (flagellar reversal regulator SadB, TypA GTPase and the PrlC oligopeptidase), were increased in
397 abundance (Table 5). The proteins showing decreased abundance included those directly associated

398 with motility (FliC, FleQ, PA0588, PchH, NuoE) and a large group of chemotaxis associated proteins
399 (PA4290, PA2867, PctB, PA2920, PA2652, PA2764, AcdB, PA0744, PA2788) and receptor protein Aer,
400 suggesting that motility was downregulated in HACs. Notably, many of these proteins are also
401 associated with biofilm formation and antibiotic resistance.

402 To elucidate the effect of hypoxia on motility further, the motility of the individual cultures was
403 assessed. The late patient strain showed a 2-fold reduction in swarming ($p<0.05$) (Fig 6B) and a
404 moderate reduction in twitching motility (1.3-fold; $p<0.01$) (Fig 6C), while H1 and H2 showed an
405 increased ability to swim (1.5 and 1.2-fold, $p<0.05$) compared to the early infection strain (Fig 6A). All
406 forms of motility were decreased in culture H3 by over 2.4-fold ($p<0.01$) (Fig 6A, 6B, 6C). A similar
407 pattern was observed in culture N3, with a 1.6-fold decrease in swimming motility ($p<0.05$) and a 1.9-
408 fold decrease in twitching motility ($p<0.01$) (Fig 6A, 6C). The pattern of swarming motility was clearly
409 different between NACs and HACs. N1 and N2 populations showed a classic swarming pattern with
410 clearly distinguishable dendrites despite showing no changes in diameter (Fig 6B). N3 showed a
411 different pattern, forming colonies with smooth edges. The H1 and H2 colonies on swarm plates were
412 clearly distinguishable from the N1 and N2 counterparts, with no clear dendrites being formed (Fig
413 6). Overall, exposure to hypoxia led to clear changes in strain motility.

414 **Figure 6. Effects of long-term hypoxia adaptation on *P. aeruginosa* motility and virulence in the *Galleria***
415 ***mellonella* model. A.** Changes in swimming motility**. B.** Changes in swarming motility. **C.** Changes in twitching
416 motility. For each type of motility, a graph representing the mean of diameter of the colony with bars
417 representing data from at least 3 separate experiments conducted in normoxic conditions, with at least two
418 technical replicates. Statistically significant difference by Kruskal-Wallis one-way ANOVA test compared to the
419 early infection strain (E) with an uncorrected Dunn's test (*$p< 0.05$; **$p< 0.01$; ***$p<0.001$; ****$p< 0.0001$).
420 **D.** Graph representing the mean CFU required to reach a lethal dose leading to 50% mortality (LD50) within
421 24h of the experiment from at least 3 independent experiments**.** A touch to the larvae head was used to
422 determine if they are alive. Statistically significant difference by Kruskal-Wallis one-way ANOVA test compared
423 to the early infection strain (E) with an uncorrected Dunn's test is presented (*$p< 0.05$). **E.** A representative
424 image showing the *G. mellonella* larvae melanisation. Healthy larvae with no disease symptoms are a bright

425 cream colour. Larvae showing a slightly beige colour show first symptoms of infection, larvae with dark
426 spots/stipes are clearly affected and the severely melanised larvae are in the late stages of the infection or
427 dead. E: early infection clinical strain; L: late infection clinical strain; N1, N2, N3: 28-day normoxia-adapted
428 populations; H1, H2, H3: 28 day hypoxia adapted populations.

429 Effects of hypoxia-adaptation on *in vivo* virulence

430 The proteome and phenotype characterisation of HACs showed that adaptation to hypoxia altered
431 the abundance of proteins involved in virulence, and the appearances of many virulence associated
432 phenotypes, including SCV formation, stress and antibiotic resistance, and motility. However,
433 unexpectedly, no differences in virulence were observed *in vivo* in *Galleria mellonella* between the
434 early infection strain and the HACs (Fig. 6D).

435

436 Discussion

437 Summary

438 Understanding the complex network of pathway interactions and the evolutionary pressures *P.*
439 *aeruginosa* undergoes in different environments is the key to understanding its biology and the
440 mechanisms behind chronic infection, facilitating the development of effective therapeutics. Hypoxic
441 niches are abundant in the CF lung due to increased mucus thickness, obstructive mucus plugging
442 and increased oxygen consumption by epithelial and immune cells (24,55,56). Studies have shown
443 that microaerobic respiration is the predominant mode of *P. aeruginosa* growth in the CF lung (57,58),
444 with two transcription factors, Anr and Dnr, tightly regulating the response to changes in oxygen
445 tension (59,60), and giving *P. aeruginosa* the ability to respond to changes in oxygen concentration
446 along a continuum (25).

447 While the impact of short-term hypoxia on *P. aeruginosa* has been previously described, the impact
448 of hypoxia stress has not been examined over extended periods. We demonstrate that prolonged low
449 oxygen conditions alone can induce stable proteomic and phenotypic changes some of which are
450 typically associated with chronic infection, and thus potentially facilitate the transition from acute to
451 chronic infection.

452 Diverse patterns of adaptation to long-term hypoxia

453 We have observed two distinct patterns of adaptation of *P. aeruginosa* to hypoxic conditions, with H1
454 and H2 adaptations being distinct from H3, which is consistent with existing literature which
455 demonstrates evolution of different phenotypic and genetic characteristics within bacterial
456 populations isolated from the same lung niche, or different parts of the biofilm, enabling bacterial
457 competitiveness (20,61–65). Flynn et. al (2006), using a similar experimental evolution approach as
458 we used in this work, albeit over 90 days, compared three biofilm cultures and three planktonic
459 cultures of *P. aeruginosa* PA14 and determined that different phenotypes appeared at different
460 intervals with different abilities to persist not only between replicate cultures, but even between
461 colonies isolated from the same population (62). Furthermore, the various colony morphologies
462 observed in this study correlated with temporal variations in c-di-GMP levels (62), which aligns with
463 the changes in the abundance of proteins associated with the response to c-di-GMP in HACs.

464 Two of the HACs in this study (H1 and H2) showed consistent alterations across multiple phenotypes,
465 while the third population displayed only slight alterations relative to the early strain and were
466 effectively comparable to the NACs (Fig. 7A). This was confirmed by a phylogenetic tree that we
467 generated based on our sequencing data (data unpublished), which showed that H1 and H2 are
468 closely related to each other, but distant from all other populations, and the third HAC was most
469 closely related to the N3 population (Fig 7B). Previous investigation of the short term hypoxia
470 response (over 24 hours) revealed that the proteome changes were strain-specific (66), suggesting

471 that different adaptation patterns can occur as the population diversifies over the longer term. A
472 further, deeper analysis of the WGS data will allow us to elucidate the genetic background of the
473 observed differences. Given the diversity of *P. aeruginosa* isolates within patients and between
474 patients, it should be noted that the late infection strain which was examined in parallel in many
475 experiments is not generally representative of late infection strains, but represents one branch with
476 a potentially more complex evolutionary tree within that patient.

477 **Figure 7. Patterns of adaptation to long-term hypoxia. A.** Summary of the phenotypic changes of adapted
478 cultures tested in normoxic conditions compared to the starting strain E and the late infection strain L. It should
479 be noted that L is a single strain and not representative of all chronic infection isolates or strains. **B.**
480 Phylogenetic tree of adapted *P. aeruginosa* populations generated by the iTOL Interactive tree of life (v6) (67).
481 The branch lengths are presented for each strain.

482 Adaptation of *Pseudomonas aeruginosa* to long-term hypoxia is consistent
483 with changes observed during chronic infection

484 Interestingly, the adaptation of *P. aeruginosa* to long-term hypoxia mirrors the phenotypic and
485 molecular changes that have been reported for *P. aeruginosa* late infection isolates as a result of
486 adaptation to chronic infection (8,18,21,23,36,65,68). These include increased SCV prevalence,
487 increased biofilm and exopolysaccharide production, increased antibiotic resistance and decreased
488 siderophore production. Importantly, it is clear that these changes are stable, as all the phenotypes
489 were tested in normoxic conditions.

490 The first phenotypic change observed during the experimental adaptation of *P. aeruginosa* to long-
491 term hypoxia was the emergence of two distinct SCV types. They were more prevalent in the HACs,
492 and one of the morphotypes was exclusive to hypoxia. Surprisingly, the abundance of c-di-GMP
493 signalling pathways proteins, Wsp, and YfiBNR, typically associated with SCVs (36,69), were
494 unchanged in the HACs, suggesting an alternative mode of regulation. SCVs are strongly associated

495 with pathogenicity and persistence among several bacterial pathogens, (70–72) and are prevalent
496 among chronic *P. aeruginosa* isolates (70,71,73). Specifically, SCVs of *P. aeruginosa* correlate with
497 increased exopolysaccharide and biofilm production, antimicrobial resistance, stress resistance and
498 host immune responses (36,73). Their emergence has been linked to redox imbalances which can be
499 caused by low oxygen conditions (74), although other environmental stressors or co-colonisation with
500 other species also contribute to their increased prevalence (70,73,75). This confirms directly, for the
501 first time, that prolonged hypoxia exposure is associated with increased SCV occurrence in *P.*
502 *aeruginosa* populations. Although SCVs temporarily occurred under normoxic conditions, they were
503 not selected as a beneficial trait in the longer term. Identification of the factors that contribute to SCV
504 emergence will be crucial due to the challenges they pose in clinical settings (70) and recognising the
505 environmental factors that select this phenotype may help us limit their occurrence.

506 Chronic infection *P. aeruginosa* CF isolates typically exhibit increased biofilm and exopolysaccharide
507 production, and reduced motility (21,65,76–78), with biofilm formation relying on hypoxia responses
508 due to the presence of steep oxygen gradients (26,79,80). Moreover, the awareness of the role of
509 biofilms in antibiotic treatment efficiency is being increasingly acknowledged (81,82).

510 The two HACs that showed a high SCV prevalence (H1, H2) also showed increased resistance to a
511 broad spectrum of antimicrobials together with increased biofilm and exopolysaccharide production.
512 Surprisingly, no trends in motility relating to hypoxia exposure or biofilm formation were observed,
513 although some changes in patterns of swarming colonies were noted.

514 Proteins associated with biofilm formation, exopolysaccharide production and motility were changed
515 in abundance, including an increase of abundance of SadB, which is required for irreversible cell
516 attachment, exopolysaccharide production and is associated with decreased swarming motility
517 (83,84), and the alternative sigma factor AlgU (σ22). AlgU is one of the key factors leading to the
518 development of chronic *P. aeruginosa* infection in the CF lung and regulates the mucoid phenotype,

519 and contributes to stress and antibiotic resistance (85–87). An interesting cascade of regulation is
520 observed, as both SadB and AlgU act through the c-di-GMP and Gac/Rsm signalling pathways (88–
521 90). Further AlgU inhibits the FleQ master regulator of flagellar motility and exopolysaccharide
522 secretion, indirectly decreasing the abundance of the FliC flagellin type B (91). Notably, another
523 modulator of the virulence, biofilm and antibiotic resistance of many Gram-negative bacteria, the
524 TypA GTPase (92,93), was also increased in abundance in HACs.

525 Antibiotic resistance is a major hallmark of *P. aeruginosa* infections in CF (94), and short-term hypoxic
526 and anaerobic conditions have been previously shown to increase *P. aeruginosa* antibiotic resistance
527 (95–97). We demonstrate that long-term exposure to hypoxia can induce stable changes in resistance
528 to antibiotics, which didn't revert following subsequent culture in normoxic conditions during
529 phenotyping or other investigations. Additionally, a wider range of proteins associated with antibiotic
530 resistance were altered in abundance, including an increase in abundance of secretion system
531 proteins and ABC transporter systems, outer membrane proteins, the TopA topoisomerase,
532 peptidoglycan/LPS biosynthesis proteins and quinolone signalling proteins. Disc diffusion assays
533 confirmed that two of the HACs showed increased resistance to a wide range of antibiotics from
534 different classes, further supporting the evidence of the extent of the influence of hypoxia pre-
535 adaptation on drug resistance and the wide range of diverse mechanisms affected.

536 Bacteria that colonise the CF lung undergo constant stress, including increased osmotic, acid and
537 oxidative stress (56,98,99). An increased resistance to oxidative stress and increased antibiotic
538 resistance was observed in two HACs, H1 and H2, which aligns with the available literature data
539 showing that preexposure to oxidative stress increases the resistance to many antibiotics (100–102).
540 Considering responses to different stress conditions involve overlapping systems (103), prolonged
541 hypoxia adaptation is likely to drive the organism's stress resistance in general. Understanding the
542 specific dynamics of this co-dependency may guide therapy choices in the future (104).

543 The airways of people with CF are reported to show an increased abundance of available iron
544 (105,106). *P. aeruginosa* expresses many iron acquisition systems including siderophore production,
545 haem acquisition systems and complexes importing iron-bound citrate or catechol (Schalk & Perraud,
546 2023). Importantly, a strong positive correlation between increased sputum iron and chronic *P.*
547 *aeruginosa* infections has been shown (108). HACs showed a decrease in the abundance of proteins
548 involved in pyochelin production (Pch cluster proteins), iron/siderophore uptake proteins/receptors
549 (FptA and ViuB), and citrate-bound iron transporter MgtA and PsfA, which alters iron uptake under
550 stress which correlate with the reports of low activity of pyochelin in CF sputum (109). The highly
551 conserved iron-sulphur cluster group, which includes the IscA and IscX (both of which were decreased
552 in abundance in HACs) is associated with iron storage and homeostasis, but also respiration, DNA and
553 RNA repair contributing to adaptation to various environments (110–112). Furthermore, iron uptake
554 and homeostasis are regulated by the c-di-GMP through the Gac/Rsm cascade (113), in line with other
555 alterations observed and underlines the role of hypoxia leading to changes in iron acquisition on
556 chronic infection development, which led to recognising them as therapy targets for *P. aeruginosa*
557 treatment (106,114).

558 It has been shown that exposure to hypoxia attenuated the virulence of isolates from acute, but not
559 chronic infections (115) and decreased their interactions with host cells, demonstrating the
560 importance of this environmental pressure. Moreover, despite the lower bacterial concentrations *in*
561 *vivo* in hypoxia, the mortality of mice was accelerated (116,117). Previous reports demonstrated that
562 decreased pyocyanin production is a characteristic of chronic infection. However, no changes in the
563 abundance of proteins associated with this phenotype were detected in HACs, and its production was
564 decreased in both HACs and NACs, suggesting that even though hypoxia may contribute to reduced
565 pyocyanin production, it is not dependent on low oxygen conditions. Additionally, we haven't
566 observed any changes in the *Galleria mellonella* infection model related to hypoxia exposure.

567 A recent study defined 224 genes of *P. aeruginosa* as pathoadaptive, and determined that the
568 expression of certain genes was associated with the host preference towards people with CF (120).
569 Nine proteins increased in abundance in HACs were encoded by pathoadaptive genes identified by
570 Weimann et al., including AlgU, FleQ, NarL, FptA, MexA, MutL, OprM, YrbF (previously discussed) and
571 additionally the RmlB rhamnose/lipopolysaccharide biosynthetic protein (121,122). Moreover, our
572 proteomics analysis showed changes in the abundance of 21 proteins encoded by genes whose
573 expression was positively associated with CF host preference and 38 that were associated with non-
574 CF infections (120), suggesting long-term hypoxia may play a role in *P. aeruginosa* infection both in CF
575 and non-CF cohorts. Although many of the phenotypes that were altered following extended
576 exposure to hypoxia can contribute to the pathogenicity of *P. aeruginosa*, the virulence of the HACs
577 was unchanged in the *G. mellonella* infection model. However, this is an acute infection model, and
578 consequently may not be optimal to assess the impact of long-term hypoxia adaptation on chronic
579 infection.

580

581 Differences between long-term adaptation and short-term response to 582 hypoxia

583 The influence of various environmental pressures on the metabolism of pathogenic bacteria is
584 typically investigated by exposing bacteria to that factor for 24 h or less, which captures early
585 responses, but it does not evaluate the prolonged environmental pressures experienced during
586 infection. No studies on the effects of long-term exposure to hypoxia have been reported in *P.*
587 *aeruginosa*, to date.

588 Our findings highlight that the bacterial strategies employed to overcome short-term and long-term
589 stress exposure are quite distinct. Short-term adaptation facilitates quick, immediate responses

590 including the stringent response and/or metabolic adjustments, whereas prolonged exposure to
591 specific conditions is more likely to foster adaptation through the acquisition and accumulation of
592 genetic changes (123–126). Specific examples include the osmotic stress response of *Pseudomonas*
593 *putida,* which initially involved upregulation of osmoprotectant production, while long-term exposure
594 led to adjustments in the outer membrane's composition to reduce permeability (103). Furthermore,
595 *Helicobacter pylori* responded to acidic stress by rapidly expressing urease to neutralise the acid, but
596 over time altered its membrane structure and proton-pumping systems (127).

597 To date, only one study has specifically investigated the global proteome changes in response to short-
598 term hypoxia studied (a few hours, until reaching OD_{600} = 1.0) (66). In contrast, to the that study,
599 which examined the *P. aeruginosa* PAO1 reference strain and two adult cystic fibrosis strains (PASS2,
600 PASS3), we used an early-infection paediatric strain (AMT 0023-30) with no prior lung adaptation,
601 providing a unique perspective (30,31,33). Only three proteins among the 101 proteins that changed
602 in abundance both after long-term and short-term hypoxia exposure were consistently altered across
603 all four strains examined in both studies, highlighting key proteins for hypoxia adaptation: the Mhr
604 microaerophilic hemerythrin and the PA0141 GDP-polyphosphate phosphotransferase were
605 increased in abundance in hypoxia, while the MaiA maleylacetoacetate isomerase decreased in
606 abundance. Their role(s) in the pathogenicity of *P. aeruginosa* suggests they may be promising
607 candidates for further studies in relation to chronic infection and its treatment (128–131). The
608 abundance of 107 proteins was altered only in long-term hypoxia cultures, but not after short-term
609 exposure. Of the 31 proteins uniquely increased in abundance during long-term adaptation, notable
610 examples previously connected to chronic infection adaptation and/or virulence include the AlgU
611 sigma factor, T6SS-associated proteins, transporters, and LPS associated proteins. Contrary to short-
612 term hypoxia exposure which led to changes in the abundance of cytochromes and denitrification
613 pathways, no changes in the abundance of these groups were detected in the long-term HACs.

614 Additionally, no increases in the abundance of proteins involved in oxidative stress resistance were
615 observed, unlike the reported short-term hypoxia response (66). This suggests that while oxidative
616 stress responses are crucial for initial response to low oxygen conditions, they are unlikely to play a
617 significant role in the adaptation to prolonged hypoxia.

618 Hypoxia-induced redox imbalance changes c-di-GMP levels

619 Hypoxia causes a redox imbalance in the bacterial cell which needs to be mitigated for the
620 maintenance of function and viability, and this process is regulated by c-di-GMP signalling. Previous
621 studies reported the role of c-di-GMP in regulating low oxygen response and stress resistance in *P.*
622 *aeruginosa* and highlight its function in the metabolic switch in response to environmental stimuli
623 including the switch from a planktonic to a biofilm lifestyle (89,132,133)**.** Moreover, the changes in c-
624 di-GMP levels were associated with diversification of populations and variability in phenotypes
625 expressed after adaptation to one condition (62). As we identified several proteins associated with
626 the GacAS system, it is tempting to speculate that hypoxia modulates the secondary messenger c-di-
627 GMP and consequently alters multiple c-di-GMP-regulated phenotypes, including the increased
628 biofilm formation and exopolysaccharide production, altered motility, and increased antibiotic
629 resistance we observed. For example, FleQ is a c-di-GMP receptor regulating biofilm formation,
630 exopolysaccharide production, and type VI secretion system expression (134–136). Considering the
631 above, we speculate that hypoxia adaptation modulates the swich from acute to chronic infection
632 through the c-di-GMP secondary messenger.

633 Common adaptation mechanisms of opportunistic pathogens to hypoxia

634 Several oxygen-sensing mechanisms, homologous genes in hypoxia regulons and several phenotypes
635 altered in chronic infection are shared across other opportunistic bacteria causing pulmonary
636 infections. This suggests that adaptation to prolonged hypoxia could be a shared mechanism between

637 many low oxygen and/or microaerophilic habitats and not limited to human infections. These
638 environments are increasingly abundant in water and soil, where opportunistic bacteria reservoirs
639 exist, and play significant roles in shaping their physiology, contributing to their increased prevalence
640 (137–141). As many opportunistic bacterial pathogens causing CF infections reside in these niches,
641 common adaptations are not unexpected.

642 Proteome analysis of HACs showed a decrease in abundance of ten proteins encoded on the Anr
643 regulon (59) that are involved in energy and amino acid metabolism (Qor, Hpd, GapN, PepN), or
644 associated with pathogenesis (LpxC – lipopolysaccharide production; ArtR – T3SS activity regulation;
645 Aer, PA2867 – chemotaxis/motility). Meanwhile, two proteins involved in biofilm production, Ppk2
646 and Mrh were increased in abundance after long-term hypoxia adaptation. Anr was reported to show
647 high activity in chronic *P. aeruginosa* infection isolates (25,26). It is noteworthy that its regulon shares
648 homologous genes with the DosR regulon of *Mycobacterium abscessus* and Lxa locus of *Burkholderia*
649 *cenocepacia*, highlighting that aspects of the hypoxia response may be shared across several
650 opportunistic CF lung infections more generally. Investigations on the impact of hypoxia on these
651 three pathogens is ongoing in our group. Targeting shared mechanisms of adaptation to chronic
652 infection could present a new opportunity for the treatment of multiple pathogens simultaneously.

653 Impact

654 Recognizing the adaptive patterns of microorganisms is critical to devising targeted treatment
655 approaches. Crucially, this study demonstrates that alterations in phenotype after long-term exposure
656 to hypoxic conditions shows several similarities with those observed by others during adaptation to
657 chronic infection. Thus, further development of our understanding of the specific mechanisms by
658 which *P. aeruginosa* adapts to hypoxia in chronic infection and the interplay with other factors present
659 in the lung environment will potentially enable us to prevent or treat the switch from acute to chronic
660 infection. This could inevitably limit antibiotic use, severity of the disease and ultimately, decrease

661 the socioeconomic impact of infections caused by *P. aeruginosa*. Furthermore, the first drug to alter
662 the human response to hypoxia was recently approved for use by the US Food and Drug
663 Administration (142). Thus it is tempting to speculate that the response of bacteria to low oxygen
664 pressures could be targeted to prevent a switch from acute to chronic infection.

665 To summarise, the changes in proteome and phenotypes (increased biofilm formation, increased
666 antibiotic resistance, decreased siderophore production, increased SCV prevalence) further deepens
667 our knowledge on how hypoxia leads to adaptation of *P. aeruginosa*, shedding light on how prolonged
668 low oxygen exposure can impact on adaptation to chronic infection and providing insights into the
669 differences between short-term responses and long-term adaptation. Overall, we confirm that
670 hypoxia contributes to multiple phenotypic changes that are prevalent in chronic infection, opening
671 a path towards designing therapies targeting these.

672

673 Materials and methods

674 Bacterial strains

675 *Pseudomonas aeruginosa* AMT 0023-30 early infection clinical strain (E) and AMT 0023-31 late
676 infection clinical strain (L) are two well characterised strains in the International *P. aeruginosa* panel
677 (31). Hypoxia- and normoxia-adapted *P. aeruginosa* strains were obtained in this study as described
678 below and are referred to as H1, H2, H3, N1, N2, and N3 (Table 1). If not stated otherwise, bacteria
679 were routinely grown in LB broth (Sigma-Aldrich, St. Louis, MO, USA) at 37°C with orbital agitation
680 (200 rpm) or plated on LB agar (Sigma-Aldrich, St. Louis, MO, USA) and grown at 37°C.

681

682 ## Experimental evolution

683 Overnight cultures of *P. aeruginosa* strain AMT 0023-30 (E) were inoculated into 30 ml LB media to
684 OD_{600} ~0.1. Prior to use, the media was equilibrated for 18 h at 37°C in an O_2 Control InVitro Glove
685 Box (PHGB model, Coy Laboratory Products, MI, United States) at 6% O_2, 5% CO_2 or in a Steri-Cycle
686 CO_2 Incubator (model 371, Thermo Scientific, Waltham, MA, USA) at 21% O_2, 5% CO_2. Three flasks
687 were inoculated as biological replicates for each of the conditions being examined. Additionally,
688 aliquots (2 ml) of the overnight *P. aeruginosa* cultures were retained as a controls for proteomic and
689 transcriptomic analysis. All flasks were incubated for 24h with agitation (200 rpm, CO_2 resistant orbital
690 shaker, model 15351105, Thermo Fisher Scientific, Waltham, MA, USA) in hypoxic and normoxic
691 conditions. Daily aliquots (2 ml) were removed for proteomic analysis from each of the flasks and also
692 additional aliquots retained for OD_{600} measurements and plating. Glycerol stocks (50%, LB (v/v)) were
693 prepared for subsequent phenotype analysis and frozen immediately to ensure minimal oxygen
694 exposure. A volume of 5% of the bacterial culture was also transferred into 30 ml of pre-equilibrated
695 media each day and this procedure was continued for up to 28 days to determine long-term
696 adaptation patterns. To ensure stability of the hypoxic conditions, all of the samples from H1, H2 and
697 H3 were taken inside the hypoxia chamber. To ensure that there were no other environmental
698 differences between the test conditions other than oxygen levels, the same batch of media was used
699 for both normoxia-adapting and hypoxia-adapting flasks and shaking conditions were consistently
700 maintained.

701 ## Whole proteome analysis

702 Samples (2 ml) were collected throughout the experimental evolution for proteome analysis. Bacterial
703 cells were pelleted at 14000-16000 g for 2 min and stored at -80°C until further analysis. Whole cell
704 lysates were extracted from each of the hypoxia- and normoxia exposed cultures by resuspending in

705 1 ml of ice-cold lysis buffer containing 40mM Tris-HCl (pH 7.8) and 1x cOmplete™, EDTA-free protease
706 inhibitor cocktail (Roche, Basel, Switzerland). Cells were disrupted by a sonication with a sonic
707 dismembrator and microtip 6mm probe (model 505; Fisherbrand, Thermo Fisher Scientific, Waltham,
708 MA, USA) (set with 20% output power using eight 10 s bursts on ice). Cell debris and any remaining
709 intact cells were pelleted using centrifugation (12000 g for 30 min). Supernatants were transferred
710 into fresh tubes and the proteins were precipitated with four volumes of methanol and incubated in
711 -80ºC overnight. The samples were centrifuged at 12000 g for 30 min at 4ºC, supernatants
712 were removed, and the protein pellets were resuspended in 200 µl of resuspension buffer containing
713 8 M urea, 50 mM Tris-HCL (pH 8.0), before 1 M 1,4-dithiothreitol (DTT) was added to each supernatant
714 (10 µl/ml lysate) and incubated at 56ºC for 30 min, followed by the addition of 1 M iodoacetamide
715 (55 µl/ml lysate) which was incubated in darkness at room temperature for 20 min. Lysates were
716 dialyzed in SnakeSkin™ tubing (Thermo Fisher Scientific, Waltham, MA, USA) with a cut-off of 3.5 kDa
717 against 100 mM ammonium bicarbonate overnight, with stirring at 4ºC, followed by at least 4 more
718 hours incubation with fresh volumes of ammonium bicarbonate. Trypsin (400 ng/µl) (Sigma-Aldrich,
719 St. Louis, MO, USA) was added to the dialyzed protein (5 µl /100 µl protein) and tubes were incubated
720 overnight at 37ºC. Aliquots from each sample were placed in fresh tubes and samples were dried in a
721 vacufuge concentrator system (model 5301; Eppendorf, Hamburg, Germany) at 65ºC and
722 resuspended in 20 µl of ZipTips resuspension buffer containing 0.5% trifluoroacetic acid (TFA) in MilliQ
723 water. ZipTips (Merc Millipore, Burlington, MA, USA) were used for peptide purification as per the
724 manufacturers' instructions. Nanodrop spectrophotometer DS-11+ (DeNovix, Wilmington, DE, USA)
725 was used for peptide concentration measurements. The samples were analysed on a Bruker TimsTOF
726 Pro mass spectrometer connected to a Evosep One chromatography system. Peptides were separated
727 on an 8 cm analytical C18 column (Evosep, 3 µm beads, 100 µm ID) using the pre-set 33 samples per
728 day gradient on the Evosep one. A trapped ion mobility (TIMS) analyser was synchronized with a
729 quadrupole mass filter to enable the highly efficient PASEF (Parallel Accumulation Serial

730 Fragmentation acquisition) procedure with acquisition rates of 100 Hz. The accumulation and ramp
731 times for the TIMS were both set to 100 ms., with an ion mobility (1/k0) range from 0.62 to 1.46
732 Vs/cm. Spectra were recorded in the mass range from 100 to 1,700 m/z. The precursor (MS) Intensity
733 Threshold was set to 2,500 and the precursor Target Intensity set to 20,000. Each PASEF cycle
734 consisted of one MS ramp for precursor detection followed by 10 PASEF MS/MS ramps, with a total
735 cycle time of 1.16 s.

736 Protein identification and label-free quantitative (LFQ) analysis were conducted using MaxQuant (v
737 2.4.2.0, https://maxquant.org/) by searching against the reference strain *P. aeruginosa* PAO1 (ATCC
738 15692). For protein identification, the following search parameters were used: trypsin was the
739 digesting enzyme with up to two missed cleavages allowed for; oxidation on methionine and
740 acetylation on the N terminus were selected as variable modifications with a fixed modification of
741 carbamidylation on cysteine; Label Free Quantitation (LFQ) and Match Between Runs (MBR) options
742 were selected. FDR for protein and peptide were set at 1%.

743 The three biological replicates from each 28 day culture condition were analysed, with one technical
744 replicate for a randomly chosen sample and LFQ intensities were compared. All missing LFQ intensities
745 were imputed with a fixed value of 1. The mean was calculated separately for the hypoxia and
746 normoxia samples, followed by fold change (FC) calculation. T-test statistical analysis was performed
747 to identify proteins with a significantly changed abundance (p-value ≤ 0.05). Proteins with a -1.5 ≤ FC
748 ≥ 1.5 were considered.

749 Functional enrichment of proteins significantly changed in abundance was performed. For GO
750 biological process functional enrichment analysis ShinyGO (v 0.80) (38) was used. Species was
751 changed to *P. aeruginosa* PAO1, FDR cutoff was set to 0.05 and the minimal pathway size was set as
752 two. For STRING local network and KEGG pathway enrichment the STRING (v 12.0) database was used
753 with default settings.

754 ## Antibiotic resistance

755 Overnight bacterial cultures were diluted in 10 ml of fresh LB to OD_{600} equal to 0.1. Bacteria were
756 spread evenly on Mueller–Hinton agar plates (Neogen, Lansing, MI, USA) using cotton swabs, in three
757 directions, to give a homogenous lawn. Antibiotic disks (Oxoid, Hampshire, UK) were placed on the
758 surface of the agar and the plates were incubated overnight in normoxic conditions at 37ºC. Growth
759 inhibition zone diameters were measured in at least two points, and the mean was used for statistical
760 analysis. The experiment was repeated three times.

761

762 ## Motility

763 Motility assays were performed as described previously (143). Swimming motility was assessed by
764 inoculating the surface of a 0.3 % (w/v) LB agar plate with overnight culture using a sterile toothpick.
765 Swimming and swarming plates were incubated overnight in normoxic conditions at 37ºC for ~18 h.
766 For swarming motility 0.8% nutrient broth (Sigma-Aldrich, St. Louis, MO, USA), 0.5% dextrose, 0.5%
767 agar plates were inoculated identically as for swimming motility assessment. The diameter of
768 bacterial growth zones was measured in at least two directions, and the mean was used for statistical
769 analysis. Twitching motility was assessed by inoculating 1.5 % (w/v) LB agar plate by piercing through
770 the agar. Plates were incubated overnight in normoxic conditions at 37ºC for ~18 h, and the agar was
771 removed. Bacteria on the surface of the plate were stained with 1% (w/v) crystal violet for 20 min.
772 The plates were washed with water until all excess dye was removed and dried at room temperature.
773 The diameter of the growth zone was measured in at least two points, and the mean was used for
774 statistical analysis. The experiment was repeated three times.

775

776 ## Biofilm production

777 Overnight cultures of *P. aeruginosa* strains were diluted in fresh LB media to OD_{600} of ~0.1, and 100 µl
778 of each diluted culture was transferred into 6 wells of a 96-well plate. The plates were incubated
779 statically in normoxic conditions at 37ºC for 24, 48 or 72 h and OD_{600} was measured with the Synergy
780 H1 microplate reader (Mason Technology, Dublin, Ireland). The medium with planktonic bacteria was
781 removed, and the biofilm fixed by incubation with 200ul of methanol for 10 min. The wells were
782 washed three times with phosphate buffered saline (PBS) (Sigma-Aldrich, St. Louis, MO, USA),
783 followed by the addition of 200 µl of 0.1% crystal violet solution and 30 min incubation at room
784 temperature. The solution was removed, and the wells were washed three times with water and once
785 with PBS. The plates were dried for at least 30 min at room temperature and 150 µl of 96% ethanol
786 was added to dissolve the bound stain. After 10 min of incubation at room temperature, the solution
787 was mixed by pipetting, OD_{590} was determined, and the OD_{590}/OD_{600} ratio was calculated. The
788 experiment was repeated three times.

789 ## Exopolysaccharide production - Congo Red agar assay

790 Overnight cultures of PA strains were pelleted and washed with 1 ml of PBS. The pellets were
791 resuspended in PBS to OD_{600} of ~0.1 and 1 µl of the suspension was plated on a Congo Red agar plate
792 (10 g/L Tryptone, 10 g/ L Bactoagar, 40mg/L Congo Red, 20mg/L Coomassie Brilliant Blue). The plates
793 were incubated for 48 h in normoxic conditions and colony morphology was assessed. The experiment
794 was repeated three times.

795 ## Stress sensitivity assays

796 Overnight cultures of PA strains were diluted to a CFU/ml of 10^8 and a range of serial dilutions was
797 prepared. Suspensions (1ul) were plated on one of the following: LB agar control plates, LB agar

798 supplemented with 0.5 M NaCl (osmotic stress), LB agar supplemented with 1mM H_2O_2 (oxidative
799 stress), or LB agar, pH 5 (acidic stress). The plates were incubated in normoxic conditions at 37°C for
800 24 or 48 h. Temperature stress was determined by incubation of an LB agar plate at 45°C for 24 h.
801 Change of sensitivity was determined by determining the lowest dilution at which bacterial growth
802 was observed. The experiment was repeated three independent times.

803 *Galleria mellonella* infection model

804 Virulence was determined as previously described (33). Wax moth larvae (*Galleria mellonella*) (The
805 KammieShop, Waalwijk, Denmark) were equilibrated in normoxic conditions at 15°C for at least 7 days
806 after arrival and stored at the same conditions for up to 4 weeks, during which larvae with a weight
807 range of 0.2-0.4 g were selected for experiments. Overnight bacterial cultures in LB were diluted in
808 fresh media to OD_{600} of ~0.1 and grown for 2-3 h. Cultures were centrifuged, and bacterial cells were
809 washed with PBS. The bacteria were diluted to 10^6 CFU/ml and serially diluted to 10^{-6}. Each dilution
810 was injected (20 µl) into the hindmost left proleg of healthy larvae (10 per group) and the same
811 volume of PBS was injected into one group as a control. Injected larvae were incubated at 37°C for
812 72 h and the number of cells causing an LD_{50} after 24 h was determined through bioburden
813 assessment by plating bacteria onto LB agar and counting colonies after 24 h. The experiment was
814 repeated at least three times for each strain tested.

815 Pyocyanin production quantification

816 *P. aeruginosa* strains were inoculated to OD_{600} in fresh PB media (20g/L Bacto-Peptone, 1.4g/L $MgCl_2$,
817 10g/L K_2SO_4) and cultured with aeration in normoxic conditions at 37°C to maximize pyocyanin
818 production. The bacterial cultures were pelleted (10 min at 12300 g) and two 7.5-ml replicates were
819 withdrawn from each of the 18 h stationary phase cultures. Pyocyanin was extracted with 4.5 ml of
820 chloroform and a total of 1.5 ml of 0.2 M HCl was added to each extract causing colour change from

821 blue to pink. The absorbance of this solution was measured at 520 nm, and the obtained values were
822 converted to pyocyanin content following Essar et al. (1990) (144). The experiment was repeated at
823 least two times.

824 Siderophore production

825 The siderophore production was quantified with a modified version of a microplate method
826 developed previously (145). Prior to siderophore quantification all glassware was rinsed with a 3M
827 solution of HCl to remove trace iron and rinsed thoroughly with deionised water. The CAS reagent
828 was prepared as described before (145).

829 Three independent cultures of each tested population or strain were grown in fresh LB medium for
830 48 h at 37°C with agitation in normoxic conditions. Aliquots of the cultures were taken for CFU counts,
831 serially diluted and plated on LB agar. The cultures were spun down (10 min at 12300 g), and 50 µl
832 aliquots of the supernatant were transferred into separate wells of a microplate followed by an
833 immediate addition of 100 µl of CAS reagent. As a control LB broth was used. The plates were
834 incubated for 20 min at room temperature in the dark and the optical density was measured at 630
835 nm using the Synergy H1 microplate reader. The Siderophore units were calculated as follows:
836 siderophore production = $[(A_{LB} - A_s) * 100]/A_{LB}$, where A_{LB} = absorbance of LB control and A_s =
837 absorbance of sample. The earlier plated bacteria were incubated at 37°C overnight and colony
838 forming units were counted. Siderophore production per colony forming unit was calculated to
839 account for any differences in growth. The experiment was repeated 2 times.

840 Determination of growth by optical density

841 To assess the influence of the inoculation volume on the growth patterns of *P. aeruginosa* AMT 0023-
842 30, 24h stationary phase cultures were inoculated into fresh LB media in a way they constituted 1%,

843 5% or 10% of the new culture. Three 200 µl technical replicates of the cultures were transferred into
844 a 96-well plate and incubated in the Synergy H1 microplate reader in normoxic conditions at 37°C
845 with agitation with OD_{600} measurements taken every 30 min.

846 Determination of growth by CFU

847 To assess the differences in the numbers of generations in hypoxic conditions and normoxic
848 conditions of the AMT0063-30 early infection strain overnight cultures were prepared. The following
849 day they were inoculated in triplicate into fresh LB media and incubated with aeration at 37°C in the
850 O_2 Control InVitro Glove Box in 6% O_2, 5% CO_2 or in 21% O_2, 5% CO_2 or in the Steri-Cycle CO_2 Incubator
851 at 21% O_2, 5% CO_2. Every hour a sample was taken from each culture for OD_{600} measurements and
852 plating on LB agar. The agar plates were incubated overnight at 37°C and the colony forming units
853 were calculated and OD_{600} to CFU/ml was plotted, a trend line was determined and R^2 calculated. The
854 doubling time was calculated for the logarithmic phase of growth using the following formula:
855 Doubling time = (Duration (min)*ln(2))/[ln(final cell concentration/initial cell concentration)].

856 Statistical analysis of phenotype data

857 Initial data preparation was performed using Microsoft Excel and statistical analysis was performed
858 using GraphPad Prism (v 8.0.2, GraphPad Software, Boston, MA, US). Only P values of 0.05 or lower
859 were considered statistically significant. First, the normality was assessed using the Shapiro-Wilk test.
860 Data with normal distribution was analysed using the Ordinary one-way ANOVA with the Uncorrected
861 Fisher's LSD; data with non-normal distribution was analysed using the Kruskal-Wallis test with an
862 uncorrected Dunn’s test. Details of the analysis and significance are provided in figure legends.

863

Acknowledgements

JD, CJC are supported by an SFI Frontiers of the Future award (20/FFP-P/8717) to SMcC. ND was supported by the Irish Research Council, GOIPG/2021/1443 IRC Award. The authors are grateful to Dr David Gomez-Matallanas for his advice in proteomic analysis and for the support of the staff and facilities in the UCD Conway proteomics core.

References

1. Antimicrobial resistance collaborators. Antimicrobial Resistance Collaborators: Global burden of bacterial antimicrobial resistance in 2019: a systematic analysis. Lancet. 2022 Feb 12;399(10325):629–55.

2. O'Neill J. Tackling drug-resistant infections globally: final report and recommendations. Wellcome Trust; 2016.

3. Blanchard AC, Waters VJ. Opportunistic Pathogens in Cystic Fibrosis: Epidemiology and Pathogenesis of Lung Infection. Journal of the Pediatric Infectious Diseases Society. 2022 Sep 1;11(Supplement_2):S3–12.

4. Sanz-García F, Gil-Gil T, Laborda P, Ochoa-Sánchez LE, Martínez JL, Hernando-Amado S. Coming from the Wild: Multidrug Resistant Opportunistic Pathogens Presenting a Primary, Not Human-Linked, Environmental Habitat. International Journal of Molecular Sciences. 2021 Jan;22(15):8080.

5. Serra-Burriel M, Keys M, Campillo-Artero C, Agodi A, Barchitta M, Gikas A, et al. Impact of multi-drug resistant bacteria on economic and clinical outcomes of healthcare-associated infections in adults: Systematic review and meta-analysis. PLoS One. 2020;15(1):e0227139.

6. Reynolds D, Kollef M. The Epidemiology and Pathogenesis and Treatment of Pseudomonas aeruginosa Infections: An Update. Drugs. 2021 Dec 1;81(18):2117–31.

7. Li Y, Roberts JA, Walker MM, Aslan AT, Harris PNA, Sime FB. The global epidemiology of ventilator-associated pneumonia caused by multi-drug resistant *Pseudomonas aeruginosa*: A systematic review and meta-analysis. International Journal of Infectious Diseases. 2024 Feb 1;139:78–85.

8. Rossi E, La Rosa R, Bartell JA, Marvig RL, Haagensen JAJ, Sommer LM, et al. Pseudomonas aeruginosa adaptation and evolution in patients with cystic fibrosis. Nat Rev Microbiol. 2021 May;19(5):331–42.

9. Smith WD, Bardin E, Cameron L, Edmondson CL, Farrant KV, Martin I, et al. Current and future therapies for Pseudomonas aeruginosa infection in patients with cystic fibrosis. FEMS Microbiology Letters. 2017 Aug 1;364(14):fnx121.

10. Botelho J, Grosso F, Peixe L. Antibiotic resistance in *Pseudomonas aeruginosa* – Mechanisms, epidemiology and evolution. Drug Resistance Updates. 2019 May 1;44:100640.

11. Bakkeren E, Diard M, Hardt WD. Evolutionary causes and consequences of bacterial antibiotic persistence. Nat Rev Microbiol. 2020 Sep;18(9):479–90.

12. Sett A, Dubey V, Bhowmik S, Pathania R. Decoding Bacterial Persistence: Mechanisms and Strategies for Effective Eradication. ACS Infect Dis. 2024 Aug;

13. ECDC. Healthcare-associated infections acquired in intensive care units - Annual Epidemiological Report for 2016. Stockholm; 2018.

14. ECDC. Healthcare-associated infections acquired in intensive care units - Annual Epidemiological Report for 2019. Stockholm; 2023.

15. Tacconelli E, Carrara E, Savoldi A, Harbarth S, Mendelson M, Monnet DL, et al. Discovery, research, and development of new antibiotics: the WHO priority list of antibiotic-resistant bacteria and tuberculosis. The Lancet Infectious Diseases. 2018 Mar 1;18(3):318–27.

16. WHO. WHO bacterial priority pathogens list, 2024: Bacterial pathogens of public health importance to guide research, development and strategies to prevent and control antimicrobial resistance. 2024.

17. Cullen L, McClean S. Bacterial Adaptation during Chronic Respiratory Infections. Pathogens. 2015 Mar;4(1):66–89.

18. Camus L, Vandenesch F, Moreau K. From genotype to phenotype: adaptations of Pseudomonas aeruginosa to the cystic fibrosis environment. Microbial Genomics. 2021;7(3):000513.

19. Chadha J, Harjai K, Chhibber S. Revisiting the virulence hallmarks of Pseudomonas aeruginosa: a chronicle through the perspective of quorum sensing. Environmental Microbiology. 2022;24(6):2630–56.

20. Cramer N, Klockgether J, Tümmler B. Microevolution of Pseudomonas aeruginosa in the airways of people with cystic fibrosis. Current Opinion in Immunology. 2023 Aug 1;83:102328.

21. Jurado-Martín I, Sainz-Mejías M, McClean S. Pseudomonas aeruginosa: An Audacious Pathogen with an Adaptable Arsenal of Virulence Factors. Int J Mol Sci. 2021 Mar 18;22(6):3128.

22. Moradali MF, Ghods S, Rehm BHA. Pseudomonas aeruginosa Lifestyle: A Paradigm for Adaptation, Survival, and Persistence. Front Cell Infect Microbiol. 2017 Feb 15;7(39).

23. Rosales-Reyes R, Vargas-Roldán SY, Lezana-Fernández JL, Santos-Preciado JI. *Pseudomonas Aeruginosa*: Genetic Adaptation, A Strategy for its Persistence in Cystic Fibrosis. Archives of Medical Research. 2021 May 1;52(4):357–61.

24. Worlitzsch D, Tarran R, Ulrich M, Schwab U, Cekici A, Meyer KC, et al. Effects of reduced mucus oxygen concentration in airway Pseudomonas infections of cystic fibrosis patients. J Clin Invest. 2002 Feb;109(3):317–25.

25. Alvarez-Ortega C, Harwood CS. Responses of Pseudomonas aeruginosa to low oxygen indicate that growth in the cystic fibrosis lung is by aerobic respiration. Molecular Microbiology. 2007;65(1):153–65.

26. Hassett DJ, Sutton MD, Schurr MJ, Herr AB, Caldwell CC, Matu JO. Pseudomonas aeruginosa hypoxic or anaerobic biofilm infections within cystic fibrosis airways. Trends in Microbiology. 2009 Mar 1;17(3):130–8.

27. Cullen L, O'Connor A, McCormack S, Owens RA, Holt GS, Collins C, et al. The involvement of the low-oxygen-activated locus of Burkholderia cenocepacia in adaptation during cystic fibrosis infection. Sci Rep. 2018 Sep 6;8(1):13386.

28. O'Connor A, Jurado-Martín I, Mysior MM, Manzira AL, Drabinska J, Simpson JC, et al. A universal stress protein upregulated by hypoxia has a role in Burkholderia cenocepacia intramacrophage survival: Implications for chronic infection in cystic fibrosis. Microbiologyopen. 2022 Dec 9;12(1):e1311.

29. Cullen L, O'Connor A, Drevinek P, Schaffer K, McClean S. Sequential Burkholderia cenocepacia Isolates from Siblings with Cystic Fibrosis Show Increased Lung Cell Attachment. Am J Respir Crit Care Med. 2017 Mar 15;195(6):832–5.

30. Mulcahy LR, Burns JL, Lory S, Lewis K. Emergence of Pseudomonas aeruginosa Strains Producing High Levels of Persister Cells in Patients with Cystic Fibrosis. Journal of Bacteriology. 2010 Oct 8;192(23):6191.

31. De Soyza A, Hall AJ, Mahenthiralingam E, Drevinek P, Kaca W, Drulis-Kawa Z, et al. Developing an international Pseudomonas aeruginosa reference panel. Microbiologyopen. 2013 Dec;2(6):1010–23.

32. Freschi L, Bertelli C, Jeukens J, Moore MP, Kukavica-Ibrulj I, Emond-Rheault JG, et al. Genomic characterisation of an international Pseudomonas aeruginosa reference panel indicates that the two major groups draw upon distinct mobile gene pools. FEMS Microbiol Lett. 2018 Jul 1;365(14).

33. Cullen L, Weiser R, Olszak T, Maldonado RF, Moreira AS, Slachmuylders L, et al. Phenotypic characterization of an international Pseudomonas aeruginosa reference panel: strains of cystic fibrosis (CF) origin show less in vivo virulence than non-CF strains. Microbiology. 2015;161(10):1961–77.

34. Aanaes K, Rickelt LF, Johansen HK, von Buchwald C, Pressler T, Høiby N, et al. Decreased mucosal oxygen tension in the maxillary sinuses in patients with cystic fibrosis. J Cyst Fibros. 2011 Mar;10(2):114–20.

35. Walkiewicz A, Brzezińska M, Bieganowski A. Methanotrophs are favored under hypoxia in ammonium-fertilized soils. Biol Fertil Soils. 2018 Oct 1;54(7):861–70.

967 36. Xu A, Zhang X, Wang T, Xin F, Ma LZ, Zhou J, et al. Rugose small colony variant and its hyper-
968 biofilm in *Pseudomonas aeruginosa*: Adaption, evolution, and biotechnological potential.
969 Biotechnology Advances. 2021 Dec 1;53:107862.

970 37. Babicki S, Arndt D, Marcu A, Liang Y, Grant JR, Maciejewski A, et al. Heatmapper: web-enabled
971 heat mapping for all. Nucleic Acids Res. 2016 Jul 8;44(W1):W147-153.

972 38. Ge SX, Jung D, Yao R. ShinyGO: a graphical gene-set enrichment tool for animals and plants.
973 Bioinformatics. 2020 Apr 15;36(8):2628–9.

974 39. Marmont LS, Rich JD, Whitney JC, Whitfield GB, Almblad H, Robinson H, et al. Oligomeric
975 lipoprotein PelC guides Pel polysaccharide export across the outer membrane of Pseudomonas
976 aeruginosa. Proceedings of the National Academy of Sciences. 2017 Mar 14;114(11):2892–7.

977 40. Poudyal B, Sauer K. The ABC of Biofilm Drug Tolerance: the MerR-Like Regulator BrlR Is an
978 Activator of ABC Transport Systems, with PA1874-77 Contributing to the Tolerance of
979 Pseudomonas aeruginosa Biofilms to Tobramycin. Antimicrobial Agents and Chemotherapy.
980 2018 Jan 25;62(2):10.1128/aac.01981-17.

981 41. Avila-Cobian LF, De Benedetti S, Kim C, Feltzer R, Champion MM, Fisher JF, et al. In vitro studies
982 of the protein-interaction network of cell-wall lytic transglycosylase RlpA of Pseudomonas
983 aeruginosa. Commun Biol. 2022 Nov 30;5(1):1–16.

984 42. Benkert B, Quäck N, Schreiber K, Jaensch L, Jahn D, Schobert M. Nitrate-responsive NarX-NarL
985 represses arginine-mediated induction of the Pseudomonas aeruginosa arginine fermentation
986 arcDABC operon. Microbiology. 2008;154(10):3053–60.

987 43. Schreiber K, Krieger R, Benkert B, Eschbach M, Arai H, Schobert M, et al. The Anaerobic
988 Regulatory Network Required for Pseudomonas aeruginosa Nitrate Respiration. Journal of
989 Bacteriology. 2007 Jun;189(11):4310–4.

990 44. Raba DA, Yuan M, Fang X, Menzer WM, Xie B, Liang P, et al. Role of Subunit D in Ubiquinone-
991 Binding Site of Vibrio cholerae NQR: Pocket Flexibility and Inhibitor Resistance. ACS Omega. 2019
992 Nov 19;4(21):19324–31.

993 45. Kotecka K, Kawalek A, Kobylecki K, Bartosik AA. The MarR-Type Regulator PA3458 Is Involved in
994 Osmoadaptation Control in Pseudomonas aeruginosa. International Journal of Molecular
995 Sciences. 2021 Jan;22(8):3982.

996 46. Aspedon A, Palmer K, Whiteley M. Microarray Analysis of the Osmotic Stress Response in
997 Pseudomonas aeruginosa. J Bacteriol. 2006 Apr;188(7):2721–5.

998 47. Wood LF, Ohman DE. Identification of Genes in the σ22 Regulon of Pseudomonas aeruginosa
999 Required for Cell Envelope Homeostasis in Either the Planktonic or the Sessile Mode of Growth.
1000 mBio. 2012 May 15;3(3):10.1128/mbio.00094-12.

1001 48. D'Souza-Ault MR, Smith LT, Smith GM. Roles of N-acetylglutaminylglutamine amide and glycine
1002 betaine in adaptation of Pseudomonas aeruginosa to osmotic stress. Appl Environ Microbiol.
1003 1993 Feb;59(2):473–8.

1004 49. Delden C van, Page MGP, Köhler T. Involvement of Fe Uptake Systems and AmpC β-Lactamase in
1005 Susceptibility to the Siderophore Monosulfactam BAL30072 in Pseudomonas aeruginosa.
1006 Antimicrobial Agents and Chemotherapy. 2013 May;57(5):2095.

1007 50. Déziel E, Gopalan S, Tampakaki AP, Lépine F, Padfield KE, Saucier M, et al. The contribution of
1008 MvfR to Pseudomonas aeruginosa pathogenesis and quorum sensing circuitry regulation:
1009 multiple quorum sensing-regulated genes are modulated without affecting lasRI, rhlRI or the
1010 production of N-acyl- l-homoserine lactones. Molecular Microbiology. 2005;55(4):998–1014.

1011 51. Irons JL, Hodge-Hanson K, Downs DM. RidA Proteins Protect against Metabolic Damage by
1012 Reactive Intermediates. Microbiology and Molecular Biology Reviews. 2020 Jul
1013 15;84(3):10.1128/mmbr.00024-20.

1014 52. Irons J, Hodge-Hanson KM, Downs DM. PA5339, a RidA Homolog, Is Required for Full Growth in
1015 Pseudomonas aeruginosa. Journal of Bacteriology. 2018 Oct 23;200(22):10.1128/jb.00434-18.

1016 53. Weiler AJ, Spitz O, Gudzuhn M, Schott-Verdugo SN, Kamel M, Thiele B, et al. A phospholipase B
1017 from *Pseudomonas aeruginosa* with activity towards endogenous phospholipids affects biofilm
1018 assembly. Biochimica et Biophysica Acta (BBA) - Molecular and Cell Biology of Lipids. 2022 Apr
1019 1;1867(4):159101.

1020 54. Yoon SS, Hennigan RF, Hilliard GM, Ochsner UA, Parvatiyar K, Kamani MC, et al. Pseudomonas
1021 aeruginosa Anaerobic Respiration in Biofilms: Relationships to Cystic Fibrosis Pathogenesis.
1022 Developmental Cell. 2002;

1023 55. König J, Schreiber R, Voelcker T, Mall M, Kunzelmann K. The cystic fibrosis transmembrane
1024 conductance regulator (CFTR) inhibits ENaC through an increase in the intracellular Cl–
1025 concentration. EMBO Rep. 2001 Nov 15;2(11):1047–51.

1026 56. Cowley ES, Kopf SH, LaRiviere A, Ziebis W, Newman DK. Pediatric Cystic Fibrosis Sputum Can Be
1027 Chemically Dynamic, Anoxic, and Extremely Reduced Due to Hydrogen Sulfide Formation. mBio.
1028 2015 Jul 28;6(4):10.1128/mbio.00767-15.

1029 57. Line L, Alhede M, Kolpen M, Kühl M, Ciofu O, Bjarnsholt T, et al. Physiological levels of nitrate
1030 support anoxic growth by denitrification of Pseudomonas aeruginosa at growth rates reported
1031 in cystic fibrosis lungs and sputum. Front Microbiol. 2014 Oct 24;5:554.

1032 58. Borriello G, Richards L, Ehrlich GD, Stewart PS. Arginine or Nitrate Enhances Antibiotic
1033 Susceptibility of Pseudomonas aeruginosa in Biofilms. Antimicrobial Agents and Chemotherapy.
1034 2006 Jan;50(1):382–4.

1035 59. Tribelli PM, Lujan AM, Pardo A, Ibarra JG, Fernández Do Porto D, Smania A, et al. Core regulon
1036 of the global anaerobic regulator Anr targets central metabolism functions in Pseudomonas
1037 species. Sci Rep. 2019 Jun 21;9(1):9065.

1038 60. Trunk K, Benkert B, Quäck N, Münch R, Scheer M, Garbe J, et al. Anaerobic adaptation in
1039 Pseudomonas aeruginosa: definition of the Anr and Dnr regulons. Environmental Microbiology.
1040 2010;12(6):1719–33.

1041 61. Ashish A, Paterson S, Mowat E, Fothergill JL, Walshaw MJ, Winstanley C. Extensive diversification
1042 is a common feature of Pseudomonas aeruginosa populations during respiratory infections in
1043 cystic fibrosis. J Cyst Fibros. 2013 Dec;12(6):790–3.

1044 62. Flynn KM, Dowell G, Johnson TM, Koestler BJ, Waters CM, Cooper VS. Evolution of Ecological
1045 Diversity in Biofilms of Pseudomonas aeruginosa by Altered Cyclic Diguanylate Signaling. Journal
1046 of Bacteriology. 2016 Sep 9;198(19):2608–18.

1047 63. Jorth P, Staudinger BJ, Wu X, Hisert K, Hayden H, Garudathri J, et al. Regional Isolation Drives
1048 Bacterial Diversification within Cystic Fibrosis Lungs. Cell Host Microbe. 2015 Sep 9;18(3):307–
1049 19.

1050 64. Markussen T, Marvig RL, Gómez-Lozano M, Aanæs K, Burleigh AE, Høiby N, et al. Environmental
1051 heterogeneity drives within-host diversification and evolution of Pseudomonas aeruginosa.
1052 mBio. 2014 Sep 16;5(5):e01592-01514.

1053 65. Winstanley C, O'Brien S, Brockhurst MA. Pseudomonas aeruginosa Evolutionary Adaptation and
1054 Diversification in Cystic Fibrosis Chronic Lung Infections. Trends Microbiol. 2016 May;24(5):327–
1055 37.

1056 66. Kamath KS, Krisp C, Chick J, Pascovici D, Gygi SP, Molloy MP. Pseudomonas aeruginosa Proteome
1057 under Hypoxic Stress Conditions Mimicking the Cystic Fibrosis Lung. J Proteome Res. 2017 Oct
1058 6;16(10):3917–28.

1059 67. Letunic I, Bork P. Interactive Tree of Life (iTOL) v6: recent updates to the phylogenetic tree display
1060 and annotation tool. Nucleic Acids Research. 2024 Jul 5;52(W1):W78–82.

1061 68. Sommer LM, Johansen HK, Molin S. Antibiotic resistance in Pseudomonas aeruginosa and
1062 adaptation to complex dynamic environments. Microbial Genomics. 2020;6(5):e000370.

1063 69. Besse A, Groleau MC, Trottier M, Vincent AT, Déziel E. Pseudomonas aeruginosa Strains from
1064 Both Clinical and Environmental Origins Readily Adopt a Stable Small-Colony-Variant Phenotype
1065 Resulting from Single Mutations in c-di-GMP Pathways. J Bacteriol. 2022 Oct
1066 18;204(10):e0018522.

1067 70. Johns BE, Purdy KJ, Tucker NP, Maddocks SE. Phenotypic and Genotypic Characteristics of Small
1068 Colony Variants and Their Role in Chronic Infection. Microbiol Insights. 2015 Jan
1069 1;8:MBI.S25800.

1070 71. Ryan H, Ballard E, Stockwell RE, Duplancic C, Thomson RM, Smith K, et al. A systematic review of
1071 the clinical impact of small colony variants in patients with cystic fibrosis. BMC Pulm Med. 2023
1072 Sep 1;23(1):323.

1073 72. Schneider M, Mühlemann K, Droz S, Couzinet S, Casaulta C, Zimmerli S. Clinical Characteristics
1074 Associated with Isolation of Small-Colony Variants of Staphylococcus aureus and Pseudomonas
1075 aeruginosa from Respiratory Secretions of Patients with Cystic Fibrosis. Journal of Clinical
1076 Microbiology. 2008 Mar 5;46(5):1832.

1077 73. Malone JG. Role of small colony variants in persistence of Pseudomonas aeruginosa infections
1078 in cystic fibrosis lungs. Infection and Drug Resistance. 2015 Jul 29;8(null):237–47.

1079 74. Besse A, Groleau MC, Déziel E. Emergence of Small Colony Variants Is an Adaptive Strategy Used
1080 by Pseudomonas aeruginosa to Mitigate the Effects of Redox Imbalance. mSphere. 2023 Feb
1081 28;8(2):e00057-23.

1082 75. Hoffman LR, Déziel E, D'Argenio DA, Lépine F, Emerson J, McNamara S, et al. Selection for
1083 Staphylococcus aureus small-colony variants due to growth in the presence of Pseudomonas
1084 aeruginosa. Proceedings of the National Academy of Sciences. 2006 Dec 26;103(52):19890–5.

1085 76. Bjarnsholt T, Jensen PØ, Fiandaca MJ, Pedersen J, Hansen CR, Andersen CB, et al. Pseudomonas
1086 aeruginosa biofilms in the respiratory tract of cystic fibrosis patients. Pediatr Pulmonol. 2009
1087 Jun;44(6):547–58.

1088 77. Høiby N, Ciofu O, Bjarnsholt T. Pseudomonas Aeruginosa Biofilms in Cystic fibrosis. Future
1089 Microbiology. 2010 Nov 1;5(11):1663–74.

1090 78. Maurice NM, Bedi B, Sadikot RT. Pseudomonas aeruginosa Biofilms: Host Response and Clinical
1091 Implications in Lung Infections. Am J Respir Cell Mol Biol. 2018 Apr;58(4):428–39.

1092 79. Klementiev AD, Jin Z, Whiteley M. Micron Scale Spatial Measurement of the O2 Gradient
1093 Surrounding a Bacterial Biofilm in Real Time. mBio. 2020 Oct 20;11(5):10.1128/mbio.02536-20.

1094 80. Wu Y, Klapper I, Stewart PS. Hypoxia arising from concerted oxygen consumption by neutrophils
1095 and microorganisms in biofilms. Pathogens and Disease. 2018 Apr 23;76(4):fty043.

1096 81. Bowler P, Murphy C, Wolcott R. Biofilm exacerbates antibiotic resistance: Is this a current
1097 oversight in antimicrobial stewardship? Antimicrob Resist Infect Control. 2020 Oct 20;9(1):162.

1098 82. Liang Z, Nilsson M, Kragh KN, Hedal I, Alcàcer-Almansa J, Kiilerich RO, et al. The role of individual
1099 exopolysaccharides in antibiotic tolerance of Pseudomonas aeruginosa aggregates. Front
1100 Microbiol. 2023 Jul 2;14(1187708).

1101 83. Caiazza NC, O'Toole GA. SadB is required for the transition from reversible to irreversible
1102 attachment during biofilm formation by Pseudomonas aeruginosa PA14. J Bacteriol. 2004
1103 Jul;186(14):4476–85.

1104 84. Caiazza NC, Merritt JH, Brothers KM, O'Toole GA. Inverse Regulation of Biofilm Formation and
1105 Swarming Motility by Pseudomonas aeruginosa PA14. J Bacteriol. 2007 May;189(9):3603–12.

1106 85. Bazire A, Shioya K, Soum-Soutéra E, Bouffartigues E, Ryder C, Guentas-Dombrowsky L, et al. The
1107 sigma factor AlgU plays a key role in formation of robust biofilms by nonmucoid Pseudomonas
1108 aeruginosa. J Bacteriol. 2010 Jun;192(12):3001–10.

1109 86. Candido Caçador N, Paulino da Costa Capizzani C, Gomes Monteiro Marin Torres LA, Galetti R,
1110 Ciofu O, da Costa Darini AL, et al. Adaptation of Pseudomonas aeruginosa to the chronic
1111 phenotype by mutations in the algTmucABD operon in isolates from Brazilian cystic fibrosis
1112 patients. PLoS One. 2018;13(11):e0208013.

1113 87. Hershberger CD, Ye RW, Parsek MR, Xie ZD, Chakrabarty AM. The algT (algU) gene of
1114 Pseudomonas aeruginosa, a key regulator involved in alginate biosynthesis, encodes an
1115 alternative sigma factor (sigma E). Proc Natl Acad Sci U S A. 1995 Aug 15;92(17):7941–5.

1116 88. Moscoso JA, Jaeger T, Valentini M, Hui K, Jenal U, Filloux A. The Diguanylate Cyclase SadC Is a
1117 Central Player in Gac/Rsm-Mediated Biofilm Formation in Pseudomonas aeruginosa. Journal of
1118 Bacteriology. 2014 Oct 29;196(23):4081–8.

1119 89. Schmidt A, Hammerbacher AS, Bastian M, Nieken KJ, Klockgether J, Merighi M, et al. Oxygen-
1120 dependent regulation of c-di-GMP synthesis by SadC controls alginate production in
1121 seudomonas aeruginosa. Environmental Microbiology. 2016;18(10):3390–402.

1122 90. Stacey SD, Pritchett CL. Pseudomonas aeruginosa AlgU Contributes to Posttranscriptional
1123 Activity by Increasing rsmA Expression in a mucA22 Strain. Journal of Bacteriology. 2016 Jun
1124 13;198(13):1812–26.

1125 91. Vijay-Kumar M, Gewirtz AT. Flagellin: key target of mucosal innate immunity. Mucosal
1126 Immunology. 2009 May 1;2(3):197–205.

1127 92. Neidig A, Yeung AT, Rosay T, Tettmann B, Strempel N, Rueger M, et al. TypA is involved in
1128 virulence, antimicrobial resistance and biofilm formation in Pseudomonas aeruginosa. BMC
1129 Microbiol. 2013 Apr 9;13(1):77.

1130 93. Overhage J, Lewenza S, Marr AK, Hancock REW. Identification of genes involved in swarming
1131 motility using a Pseudomonas aeruginosa PAO1 mini-Tn5-lux mutant library. J Bacteriol. 2007
1132 Mar;189(5):2164–9.

1133 94. Sindeldecker D, Stoodley P. The many antibiotic resistance and tolerance strategies of
1134 *Pseudomonas aeruginosa*. Biofilm. 2021 Dec 1;3:100056.

1135 95. Borriello G, Werner E, Roe F, Kim AM, Ehrlich GD, Stewart PS. Oxygen Limitation Contributes to
1136 Antibiotic Tolerance of Pseudomonas aeruginosa in Biofilms. Antimicrobial Agents and
1137 Chemotherapy. 2004 Jul;48(7):2659–64.

1138 96. Schaible B, Taylor CT, Schaffer K. Hypoxia Increases Antibiotic Resistance in Pseudomonas
1139 aeruginosa through Altering the Composition of Multidrug Efflux Pumps. Antimicrobial Agents
1140 and Chemotherapy. 2012 Mar 16;56(4):2114–8.

1141 97. Zhao X, Drlica K. Reactive oxygen species and the bacterial response to lethal stress. Current
1142 opinion in microbiology. 2014 Jul 30;0:1.

1143 98. Puchelle E, Bajolet O, Abély M. Airway mucus in cystic fibrosis. Paediatric Respiratory Reviews.
1144 2002 Jun 1;3(2):115–9.

1145 99. Bhagirath AY, Li Y, Somayajula D, Dadashi M, Badr S, Duan K. Cystic fibrosis lung environment and
1146 Pseudomonas aeruginosa infection. BMC Pulm Med. 2016 Dec 5;16:174.

1147 100. Lan L, Murray TS, Kazmierczak BI, He C. Pseudomonas aeruginosa OspR is an oxidative stress
1148 sensing regulator that affects pigment production, antibiotic resistance and dissemination
1149 during infection. Molecular Microbiology. 2010;75(1):76–91.

1150 101. Fraud S, Poole K. Oxidative Stress Induction of the MexXY Multidrug Efflux Genes and Promotion
1151 of Aminoglycoside Resistance Development in Pseudomonas aeruginosa. Antimicrobial Agents
1152 and Chemotherapy. 2011 Feb 24;55(3):1068–74.

102. Mohamed FA, Shaker GH, Askoura MM. Oxidative Stress Influences Pseudomonas aeruginosa Susceptibility to Antibiotics and Reduces Its Pathogenesis in Host. Curr Microbiol. 2020 Mar 1;77(3):479–90.

103. Bojanovič K, D'Arrigo I, Long KS. Global Transcriptional Responses to Osmotic, Oxidative, and Imipenem Stress Conditions in Pseudomonas putida. Applied and Environmental Microbiology. 2017 Mar 17;83(7):e03236.

104. Dawan J, Ahn J. Bacterial Stress Responses as Potential Targets in Overcoming Antibiotic Resistance. Microorganisms. 2022 Jul;10(7):1385.

105. Hunter RC, Asfour F, Dingemans J, Osuna BL, Samad T, Malfroot A, et al. Ferrous Iron Is a Significant Component of Bioavailable Iron in Cystic Fibrosis Airways. mBio. 2013 Aug 20;4(4):10.1128/mbio.00557-13.

106. Moreau-Marquis S, Bomberger JM, Anderson GG, Swiatecka-Urban A, Ye S, O'Toole GA, et al. The DeltaF508-CFTR mutation results in increased biofilm formation by Pseudomonas aeruginosa by increasing iron availability. Am J Physiol Lung Cell Mol Physiol. 2008 Jul;295(1):L25-37.

107. Schalk IJ, Perraud Q. and its multiple strategies to access iron. Environmental Microbiology. 2023;25(4):811–31.

108. Reid DW, Carroll V, O'May C, Champion A, Kirov SM. Increased airway iron as a potential factor in the persistence of Pseudomonas aeruginosa infection in cystic fibrosis. European Respiratory Journal. 2007 Aug 1;30(2):286–92.

109. Konings AF, Martin LW, Sharples KJ, Roddam LF, Latham R, Reid DW, et al. Pseudomonas aeruginosa Uses Multiple Pathways To Acquire Iron during Chronic Infection in Cystic Fibrosis Lungs. Infection and Immunity. 2013 Jul 11;81(8):2697–704.

110. Lo Sciuto A, D'Angelo F, Spinnato MC, Garcia PS, Genah S, Matteo C, et al. A molecular comparison of [Fe-S] cluster-based homeostasis in Escherichia coli and Pseudomonas aeruginosa. mBio. 2024 Oct 3;0(0):e01206-24.

111. Py B, Barras F. Building Fe–S proteins: bacterial strategies. Nat Rev Microbiol. 2010 Jun;8(6):436–46.

112. Romsang A, Duang-Nkern J, Leesukon P, Saninjuk K, Vattanaviboon P, Mongkolsuk S. The Iron-Sulphur Cluster Biosynthesis Regulator IscR Contributes to Iron Homeostasis and Resistance to Oxidants in Pseudomonas aeruginosa. PLOS ONE. 2014 sty;9(1):e86763.

113. Frangipani E, Visaggio D, Heeb S, Kaever V, Cámara M, Visca P, et al. The Gac/Rsm and cyclic-di-GMP signalling networks coordinately regulate iron uptake in seudomonas aeruginosa. Environmental Microbiology. 2014;16(3):676–88.

114. Banin E, Brady KM, Greenberg EP. Chelator-induced dispersal and killing of Pseudomonas aeruginosa cells in a biofilm. Appl Environ Microbiol. 2006 Mar;72(3):2064–9.

115. Schaible B, Rodriguez J, Garcia A, von Kriegsheim A, McClean S, Hickey C, et al. Hypoxia Reduces the Pathogenicity of Pseudomonas aeruginosa by Decreasing the Expression of Multiple Virulence Factors. J Infect Dis. 2017 May 1;215(9):1459–67.

116. Gil-Marqués ML, Pachón-Ibáñez ME, Pachón J, Smani Y. Effect of Hypoxia on the Pathogenesis of Acinetobacter baumannii and Pseudomonas aeruginosa In Vitro and in Murine Experimental Models of Infection. Infection and Immunity. 2018 Sep 21;86(10):10.1128/iai.00543-18.

117. Schaible B, McClean S, Selfridge A, Broquet A, Asehnoune K, Taylor CT, et al. Hypoxia Modulates Infection of Epithelial Cells by Pseudomonas aeruginosa. PLOS ONE. 2013 Feb 13;8(2):e56491.

118. Jiao H, Li F, Wang T, Yam JKH, Yang L, Liang H. The Pyocin Regulator PrtR Regulates Virulence Expression of Pseudomonas aeruginosa by Modulation of Gac/Rsm System and c-di-GMP Signaling Pathway. Infection and Immunity. 2021 Jan 19;89(2).

119. Vilaplana L, Marco MP. Phenazines as potential biomarkers of Pseudomonas aeruginosa infections: synthesis regulation, pathogenesis and analytical methods for their detection. Anal Bioanal Chem. 2020 Sep 1;412(24):5897–912.

120. Weimann A, Dinan AM, Ruis C, Bernut A, Pont S, Brown K, et al. Evolution and host-specific adaptation of Pseudomonas aeruginosa. Science. 2024 Jul 5;385(6704):eadi0908.

121. Aguirre-Ramírez M, Medina G, González-Valdez A, Grosso-Becerra V, Soberón-Chávez G. The Pseudomonas aeruginosa rmlBDAC operon, encoding dTDP-l-rhamnose biosynthetic enzymes, is regulated by the quorum-sensing transcriptional regulator RhlR and the alternative sigma factor σS. Microbiology. 2012;158(4):908–16.

122. Rahim R, Burrows LL, Monteiro MA, Perry MB, Lam JS. Involvement of the rml locus in core oligosaccharide and O polysaccharide assembly in Pseudomonas aeruginosa. Microbiology. 2000;146(11):2803–14.

123. Koska M, Kordes A, Erdmann J, Willger SD, Thöming JG, Bähre H, et al. Distinct Long- and Short-Term Adaptive Mechanisms in Pseudomonas aeruginosa. Microbiology Spectrum. 2022 Nov 14;10(6):e03043-22.

124. McHugh JP, Rodríguez-Quiñones F, Abdul-Tehrani H, Svistunenko DA, Poole RK, Cooper CE, et al. Global Iron-dependent Gene Regulation in *Escherichia coli*. Journal of Biological Chemistry. 2003 Aug 8;278(32):29478–86.

125. Touati D. Iron and oxidative stress in bacteria. Arch Biochem Biophys. 2000 Jan 1;373(1):1–6.

126. Zhang Y, Zhang X, Zhang H, He Q, Zhou Q, Su Z, et al. Responses of Soil Bacteria to Long-Term and Short-Term Cadmium Stress as Revealed by Microbial Community Analysis. Bull Environ Contam Toxicol. 2009 Mar 1;82(3):367–72.

127. Krulwich TA, Sachs G, Padan E. Molecular aspects of bacterial pH sensing and homeostasis. Nature reviews Microbiology. 2011 Apr 5;9(5):330.

128. Clay ME, Hammond JH, Zhong F, Chen X, Kowalski CH, Lee AJ, et al. Pseudomonas aeruginosa lasR mutant fitness in microoxia is supported by an Anr-regulated oxygen-binding hemerythrin. Proc Natl Acad Sci U S A. 2020 Feb 11;117(6):3167–73.

1227 129. Neville N, Roberge N, Ji X, Stephen P, Lu JL, Jia Z. A Dual-Specificity Inhibitor Targets
1228 Polyphosphate Kinase 1 and 2 Enzymes To Attenuate Virulence of Pseudomonas aeruginosa.
1229 mBio. 2021 Jun 15;12(3):e00592.

1230 130. Ortiz-Severín J, Varas M, Bravo-Toncio C, Guiliani N, Chávez FP. Multiple antibiotic susceptibility
1231 of polyphosphate kinase mutants (ppk1 and ppk2) from Pseudomonas aeruginosa PAO1 as
1232 revealed by global phenotypic analysis. biol res. 2015 Apr 25;48(1):22.

1233 131. Salunkhe P, Smart CHM, Morgan JAW, Panagea S, Walshaw MJ, Hart CA, et al. A Cystic Fibrosis
1234 Epidemic Strain of Pseudomonas aeruginosa Displays Enhanced Virulence and Antimicrobial
1235 Resistance. Journal of Bacteriology. 2005 Jul;187(14):4908–20.

1236 132. An S, Wu J, Zhang LH. Modulation of Pseudomonas aeruginosa Biofilm Dispersal by a Cyclic-Di-
1237 GMP Phosphodiesterase with a Putative Hypoxia-Sensing Domain. Appl Environ Microbiol. 2010
1238 Dec;76(24):8160–73.

1239 133. Feng Q, Zhou J, Zhang L, Fu Y, Yang L. Insights into the molecular basis of c-di-GMP signalling in
1240 Pseudomonas aeruginosa. Critical Reviews in Microbiology. 2024 Jan 2;50(1):20–38.

1241 134. Hickman JW, Harwood CS. Identification of FleQ from Pseudomonas aeruginosa as a c-di-GMP-
1242 responsive transcription factor. Mol Microbiol. 2008 Jul;69(2):376–89.

1243 135. Matsuyama BY, Krasteva PV, Baraquet C, Harwood CS, Sondermann H, Navarro MVAS.
1244 Mechanistic insights into c-di-GMP-dependent control of the biofilm regulator FleQ from
1245 Pseudomonas aeruginosa. Proc Natl Acad Sci U S A. 2016 Jan 12;113(2):E209-218.

1246 136. Zhou T, Huang J, Liu Z, Lin Q, Xu Z, Zhang LH. The Two-Component System FleS/FleR Represses
1247 H1-T6SS via Cyclic di-GMP Signaling in Pseudomonas aeruginosa. Appl Environ Microbiol. 2022
1248 Jan 25;88(2):e0165521.

1249 137. Amoureux L, Bador J, Fardeheb S, Mabille C, Couchot C, Massip C, et al. Detection of
1250 Achromobacter xylosoxidans in Hospital, Domestic, and Outdoor Environmental Samples and
1251 Comparison with Human Clinical Isolates. Appl Environ Microbiol. 2013 Dec;79(23):7142–9.

1252 138. Crone S, Vives-Flórez M, Kvich L, Saunders AM, Malone M, Nicolaisen MH, et al. The
1253 environmental occurrence of Pseudomonas aeruginosa. APMIS. 2020;128(3):220–31.

1254 139. Honda JR, Virdi R, Chan ED. Global Environmental Nontuberculous Mycobacteria and Their
1255 Contemporaneous Man-Made and Natural Niches. Front Microbiol. 2018 Aug 30;9.

1256 140. Honda JR, Virdi R, Chan ED. Global Environmental Nontuberculous Mycobacteria and Their
1257 Contemporaneous Man-Made and Natural Niches. Front Microbiol. 2018;9:2029.

1258 141. Price CTD, Hanford HE, Al-Quadan T, Santic M, Shin CJ, Da'as MSJ, et al. Amoebae as training
1259 grounds for microbial pathogens. mBio. 2024 Jul 8;15(8):e00827-24.

1260 142. Mullard A. 2023 FDA approvals. Nat Rev Drug Discov. 2024 Feb;23(2):88–95.

1261 143. Rashid MH, Kornberg A. Inorganic polyphosphate is needed for swimming, swarming, and
1262 twitching motilities of Pseudomonas aeruginosa. Proc Natl Acad Sci U S A. 2000 Apr
1263 25;97(9):4885–90.

144. Essar DW, Eberly L, Hadero A, Crawford IP. Identification and characterization of genes for a second anthranilate synthase in Pseudomonas aeruginosa: interchangeability of the two anthranilate synthases and evolutionary implications. J Bacteriol. 1990 Feb;172(2):884–900.

145. Arora NK, Verma M. Modified microplate method for rapid and efficient estimation of siderophore produced by bacteria. 3 Biotech. 2017 Dec;7(6):381.

Supporting information captions

S1. Figure. Differences in growth patterns of the *P. aeruginosa* AMT 0023-30 early infection strain with different inoculation volumes.

S2. Figure. Differences in doubling times of the *P. aeruginosa* AMT 002330 early infection strain in hypoxic and normoxic conditions. A. OD_{600} measurements over time. **B.** CFU/ml counts over time **C.** OD_{600} to CFU/ml trend lines and linear regression calculations. **D.** Differences in generation times in normoxia and hypoxia.

S3. Table. All proteins showing significant changes in abundance after 28 day exposure to hypoxia

S4. Table. Functional enrichment of proteins changed in abundance after 28 days of exposure to hypoxia

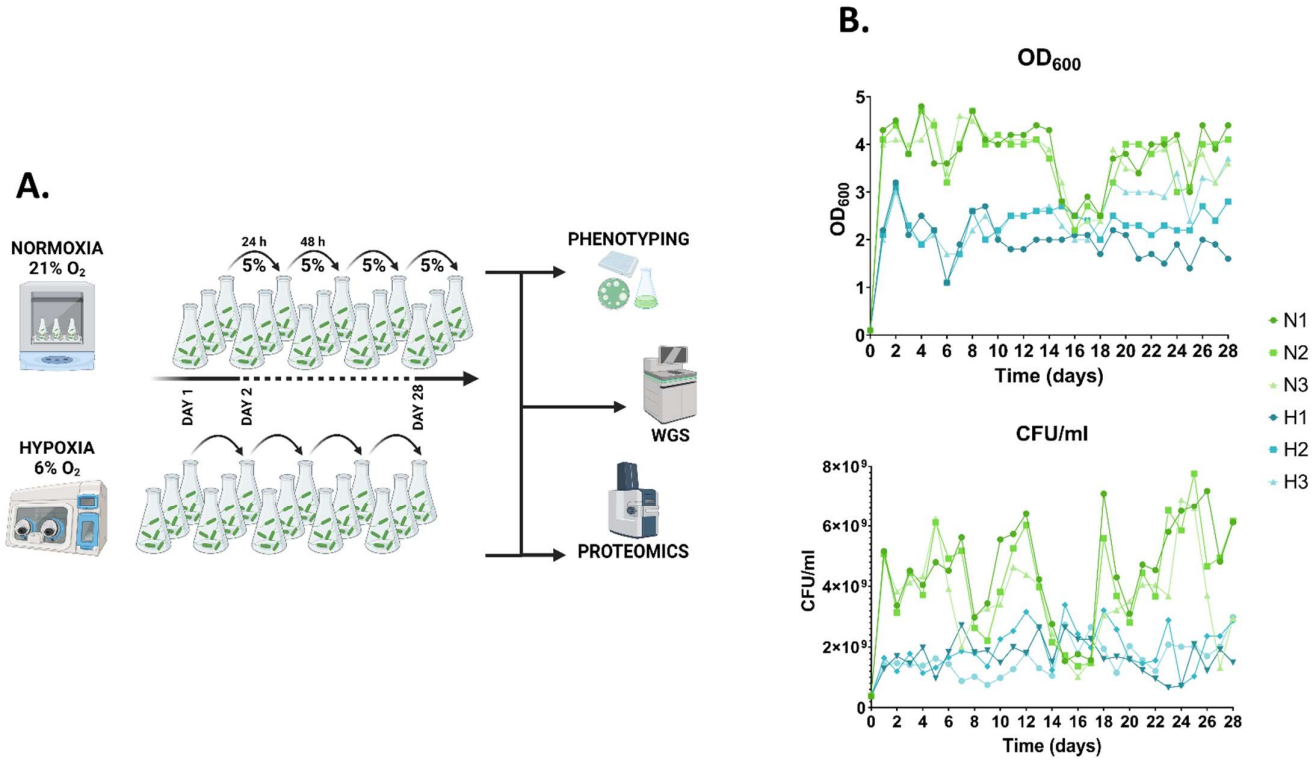

Figure 1. Long-term adaptation of *Pseudomonas aeruginosa* to hypoxic conditions. A. Experimental evolution design. **B.** OD_{600} changes and CFU/ml count changes over the 28 days of the long-term adaptation study

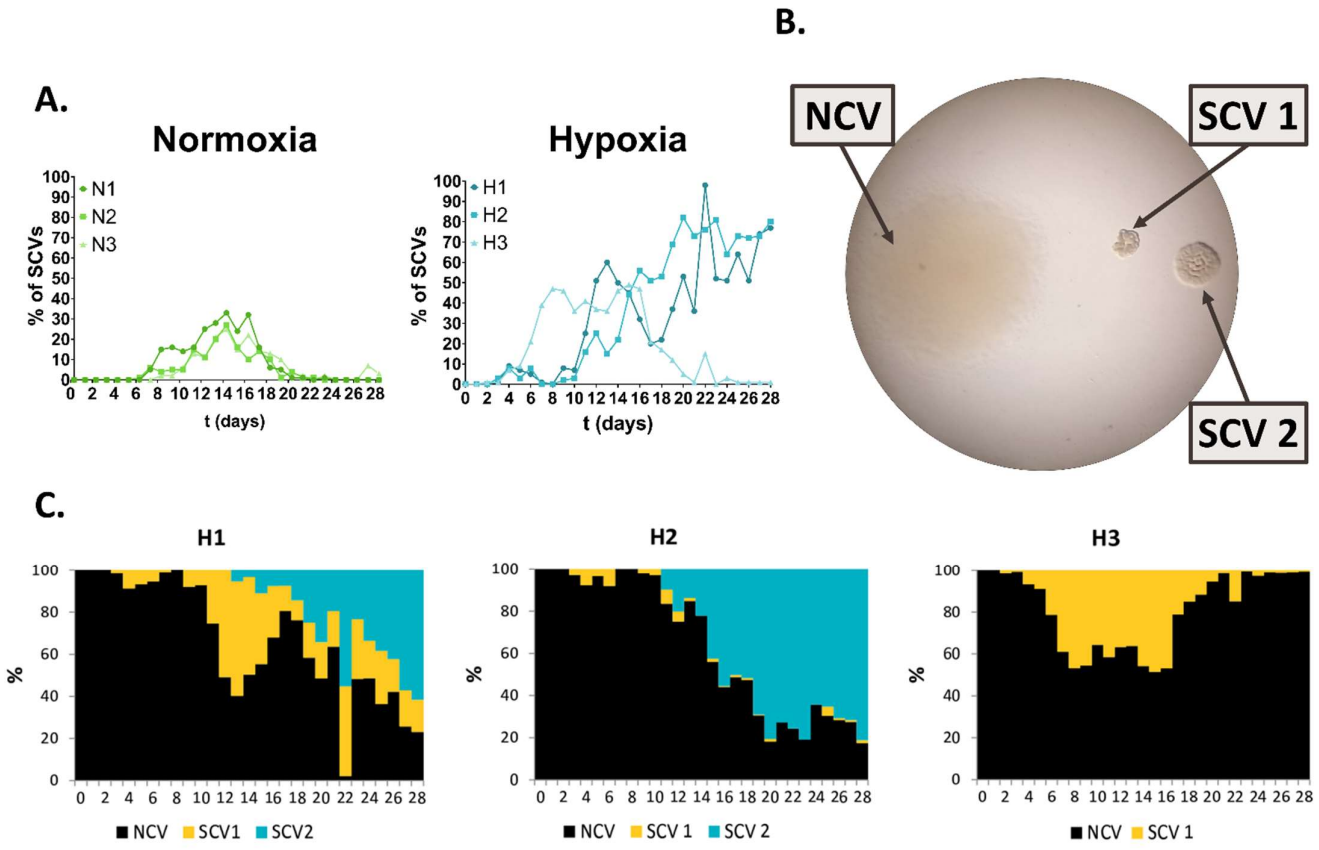

Figure 2. Influence of hypoxia on small colony variants emergence. A. Percentage of SCVs in individual normoxia- and hypoxia adapting cultures over 28 days. **B.** Hypoxia-adapted colony morphotypes observed throughout the long-term adaptation **C.** Ratios of the different colony morphotypes in the hypoxia-adapting populations over 28 days. The percentage of the small colony variants in the whole populations was caried out for each flask individually each day of the experiment.

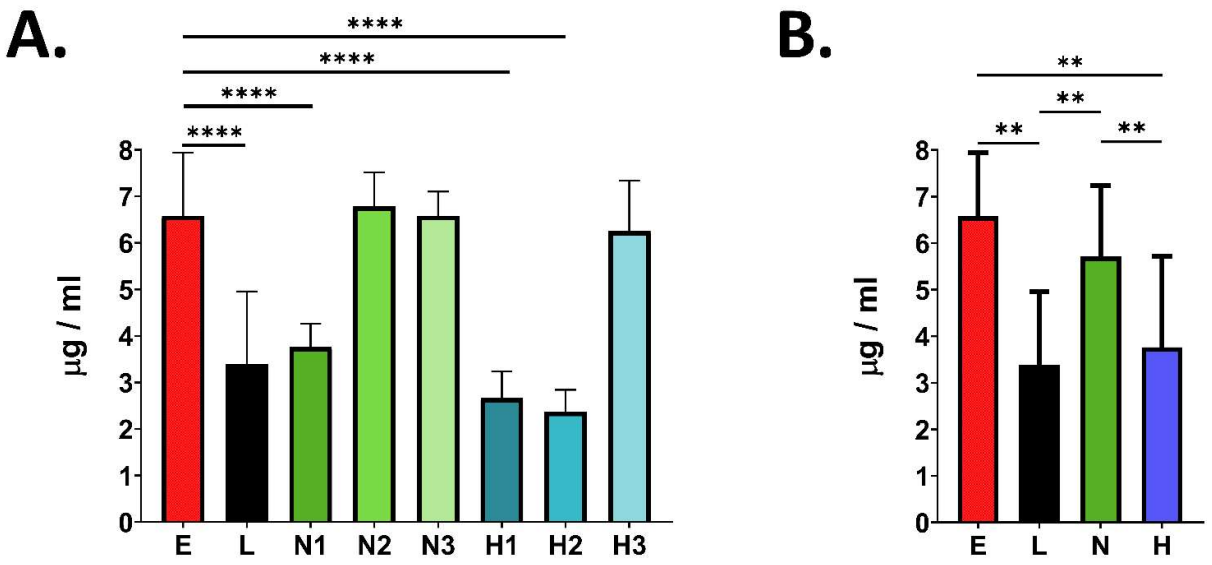

Fig. 3 Influence of hypoxia on pyocyanin production by individual populations **(A.)** or representing the pooled data for normoxia- and hypoxia-adapted cultures (**B.**). The data represents the concentration of pyocyanin in 1ml of bacterial culture, calculated as described in the methods. The data represents two separate experiments with at least 3 technical replicates for each strain. Statistically significant differences by ordinary one-way ANOVA test compared to the early infection strain with an uncorrected Fishers LSD test (A) or Kurskal-Wallis one-way ANOVA test comparing all groups with an uncorrected Dunn's test (B) are shown (**p< 0.01; ***p<0.001; ****p< 0.0001). E: early infection clinical isolate; L: late infection clinical isolate; N1, N2, N3: 28-day normoxia-adapted populations; H1, H2, H3: 28-day hypoxia adapted populations.

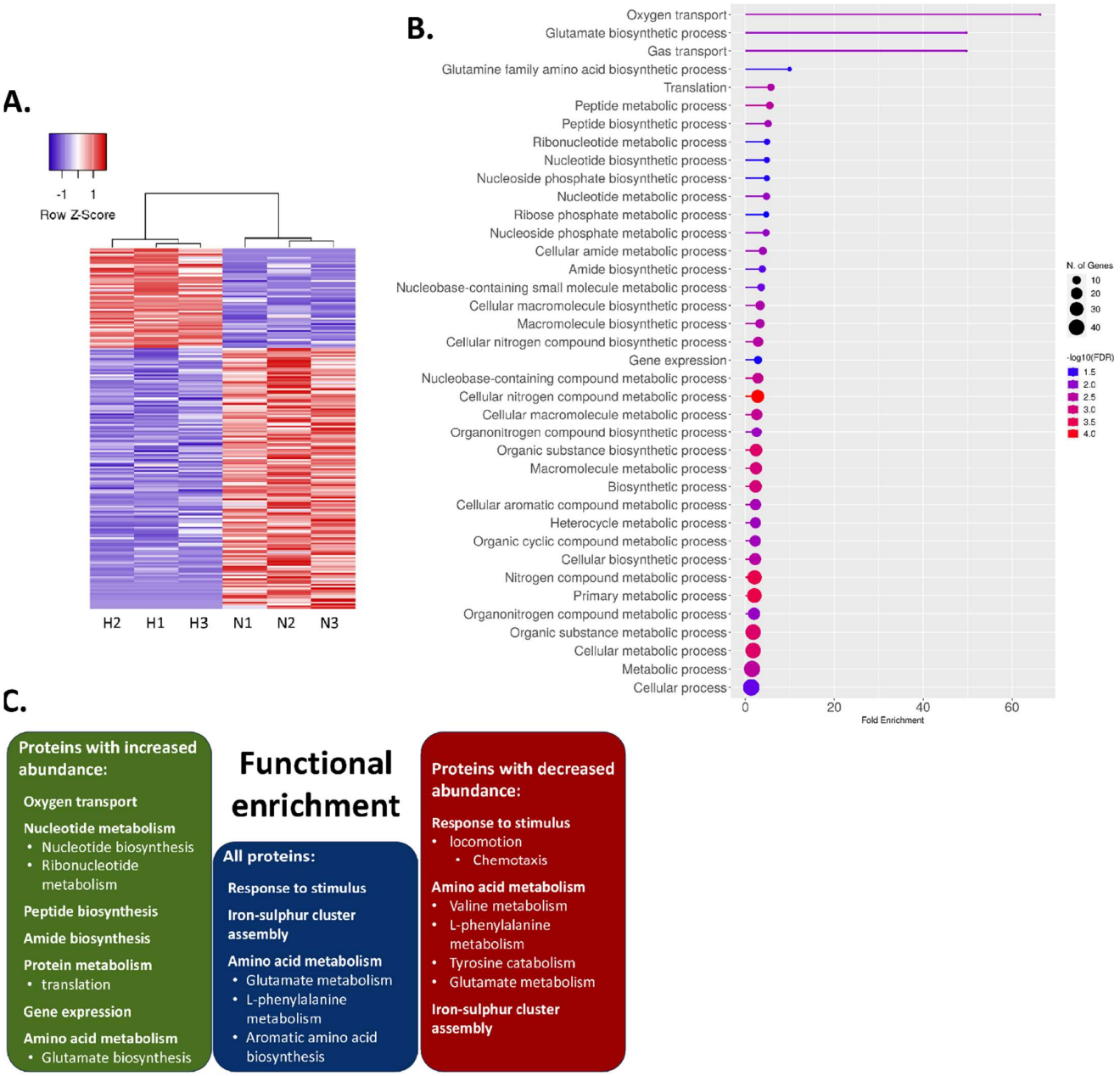

Figure 4. Whole proteome comparison of long-term hypoxia-adapted and normoxia-adapted *P. aeruginosa.* **A.** Heat map representing expression patterns in adapted populations. The heatmap was generated with the use of Heatmapper (Babicki et al., 2016). **B.** Dot plot representing functional GoTerm Biological Process enrichment of proteins with increased and decreased abundance in hypoxia. The enrichment analysis and dot plot were prepared using ShinyGo 0.80. v. ???. Statistics? Edit picture

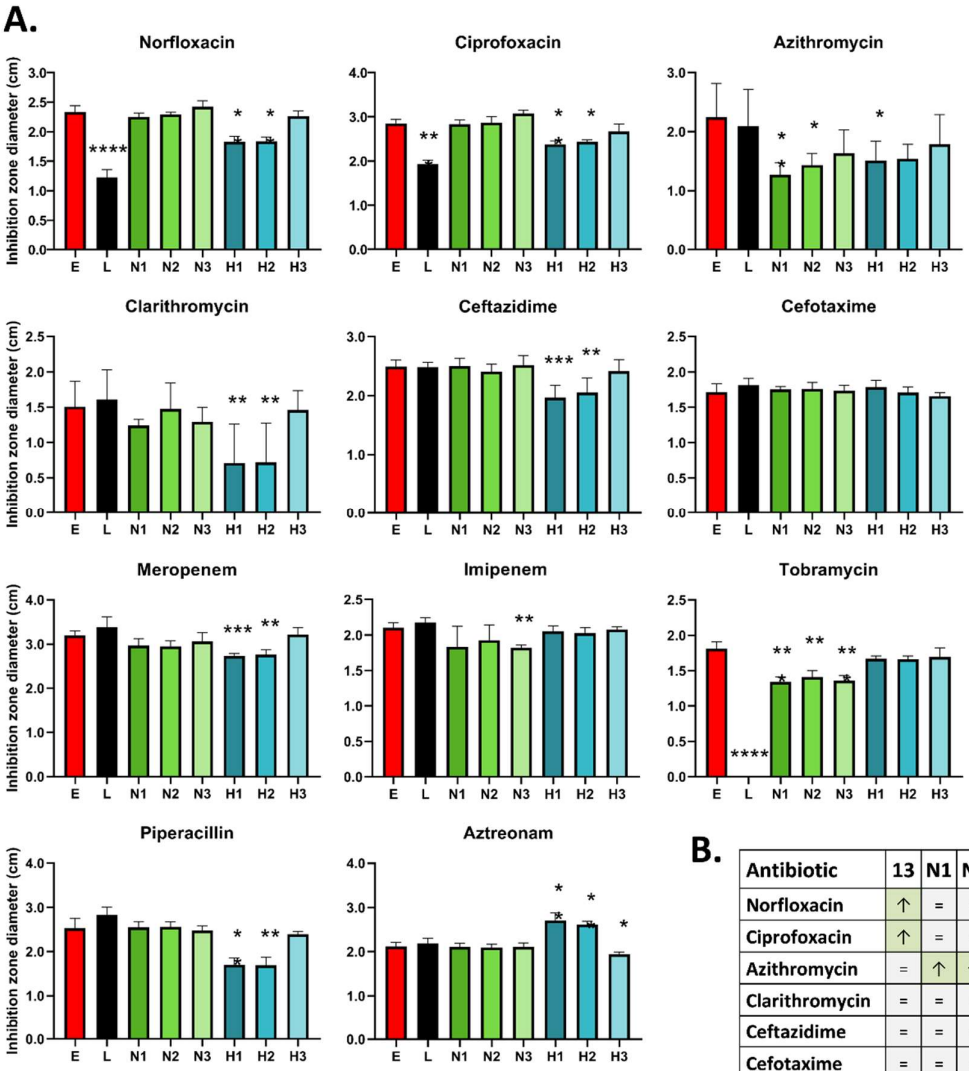

B.

Antibiotic	13	N1	N2	N3	H1	H2	H3	Antibiotic Class
Norfloxacin	↑	=	=	=	↑	↑	=	Fluoroquinolones
Ciprofoxacin	↑	=	=	=	↑	↑	=	
Azithromycin	=	↑	↑	=	↑	=	=	Macrolides
Clarithromycin	=	=	=	=	↑	↑	=	
Ceftazidime	=	=	=	=	↑	↑	=	Cephalosporins
Cefotaxime	=	=	=	=	=	=	=	
Meropenem	=	=	=	=	↑	↑	=	Carbapenems
Imipenem	=	=	=	↑	=	=	=	
Tobramycin	↑R	↑	↑	↑	=	=	=	Aminoglycosides
Piperacillin	↓	=	=	=	↑	↑	=	Penicillins
Aztreonam	=	=	=	=	↓	↓	↑	Monobactams
Tetracycline	= R	= R	= R	= R	= R	= R	= R	Tetracyclines

Figure 5. Effects of long-term hypoxia adaptation on antibiotic sensitivity. **A.** Graphs represent the antibiotic susceptibility of early infection control strain, late infection strain, and 28-day adapted populations using diffusion discs. Bars represent the mean inhibition zone diameter. The data represents 3 biological replicates and error bars represent the standard deviation. The significance was determined with the nonparametric Kurskal-Wallis test in combination with uncorrected Dunns multiple comparisons test. **B**. Summary of resistance to all tested antibiotics. ↑ - increased resistance; ↓ - decreased resistance; = no significant difference in resistance; R – no inhibition zone observed. E: early infection clinical isolate; L: late infection clinical isolate; N1, N2, N3: 28-day normoxia-adapted populations; H1, H2, H3: 28-day hypoxia adapted populations.

A.

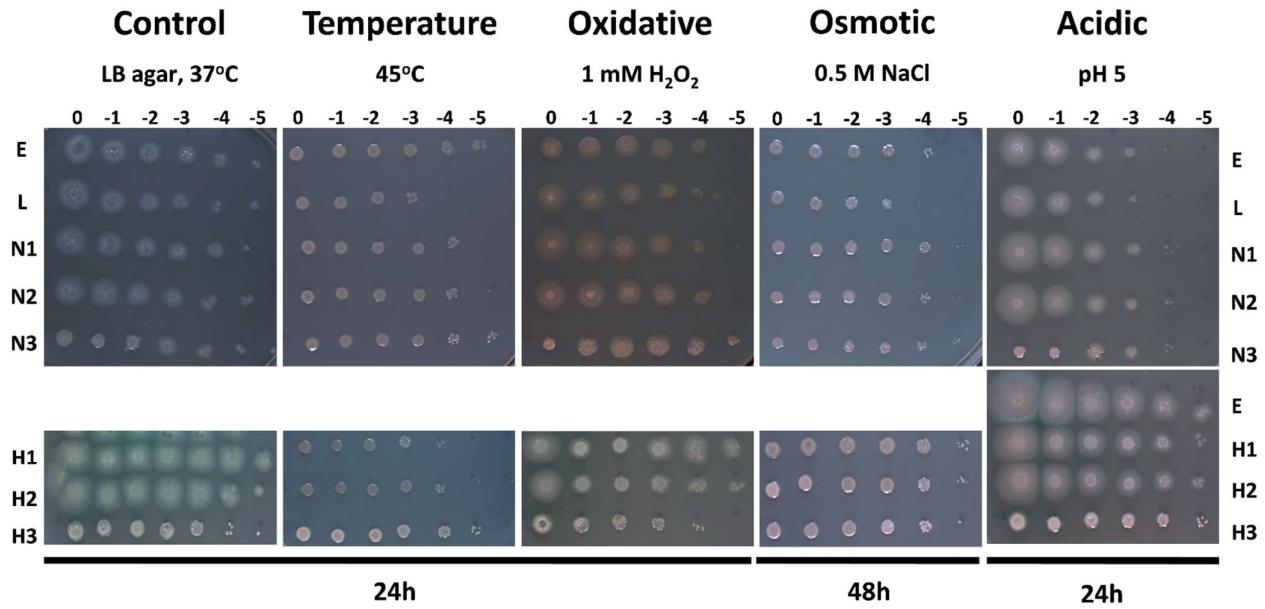

B.

Stress type	L	N1	N2	N3	H1	H2	H3
Temperature	↓	↓	↓	=	↓	↓	=
Osmotic	↓	↑	=	↑	↑	↑	↑
Oxidative	=	=	=	↑	↑	↑	=
Acidic	=	↑	↑	↑	=	=	=

Figure 6. Effects of long-term hypoxia adaptation on stress sensitivity. **A.** Droplet assays. Representative pictures of colonies from serial dilutions of each strain plated on agar with stress factor added. The experiment was repeated at least 3 times for each stress type with the early infection isolate as a control. **B.** Table summarising changes in stress sensitivity. E: early infection clinical isolate; L: late infection clinical isolate; N1, N2, N3: 28-day normoxia-adapted populations; H1, H2, H3: 28-day hypoxia adapted populations

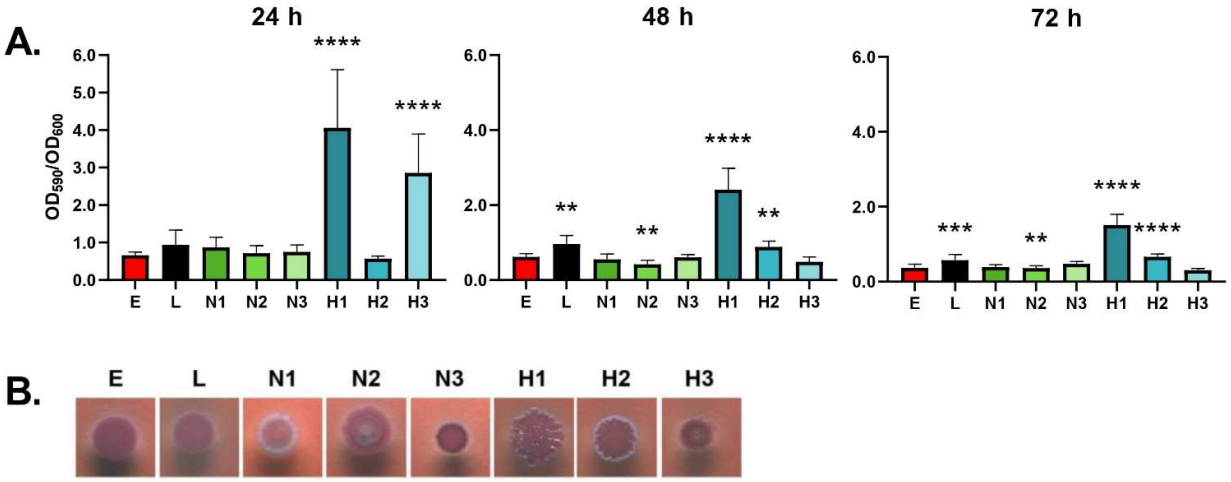

Figure 7. Effects of long-term hypoxia adaptation on biofilm formation and exopolysaccharide production. A. Biofilm formation capability of hypoxia-adapted cultures determined with the crystal violet assay after 24, 48 or 72h of static incubation on a 96-well plate. Data represents the mean value of the OD_{590}/OD_{600} ratio from three separate experiments with at least 6 technical replicates for each strain. Statistically significant difference by Kurskal-Wallis one-way ANOVA test compared to the early infection strain (E) with an uncorrected Dunn's test (**p< 0.01; ***p<0.001; ****p< 0.0001). **B.** Exopolysaccharide production by the adapted cultures. The photographs show colonies of different populations of bacteria. The change of colour to a darker shade and a wrinkly colony surface indicate a higher exopolysaccharide production. E: early infection clinical isolate; L: late infection clinical isolate; N1, N2, N3: 28-day normoxia-adapted populations; H1, H2, H3: 28-day hypoxia adapted populations

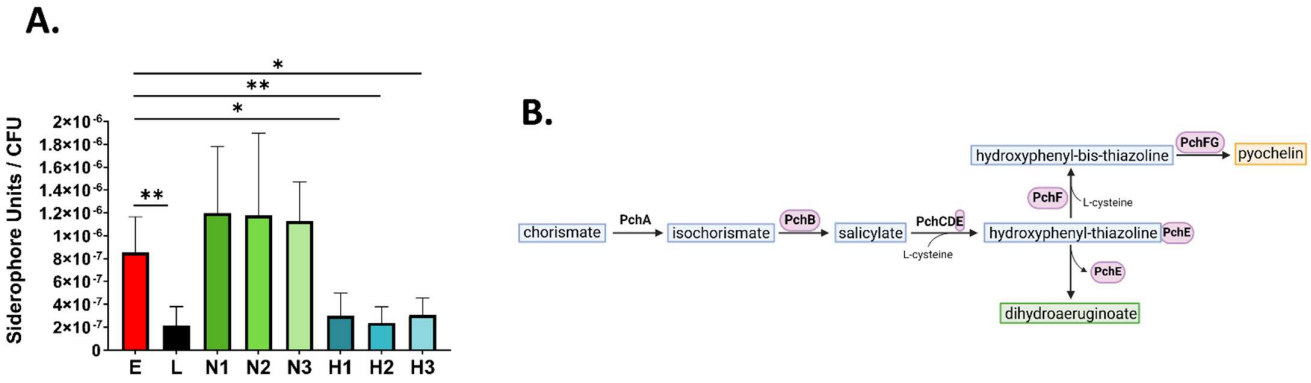

Fig. 8. Effects of long-term hypoxia adaptation on siderophore production. A. Siderophore production represented as an average of siderophore units produced by each colony forming unit. Statistically significant differences by ordinary one-way ANOVA test compared to the early infection strain with an uncorrected Fishers LSD test (are shown (*p<0.05; **p< 0.01). E: early infection clinical isolate; L: late infection clinical isolate; N1, N2, N3: 28-day normoxia-adapted populations; H1, H2, H3: 28-day hypoxia adapted populations. **B.** Pathway of pyochelin synthesis. Pink – proteins decreased in abundance in the proteome of hypoxia-adapted populations.

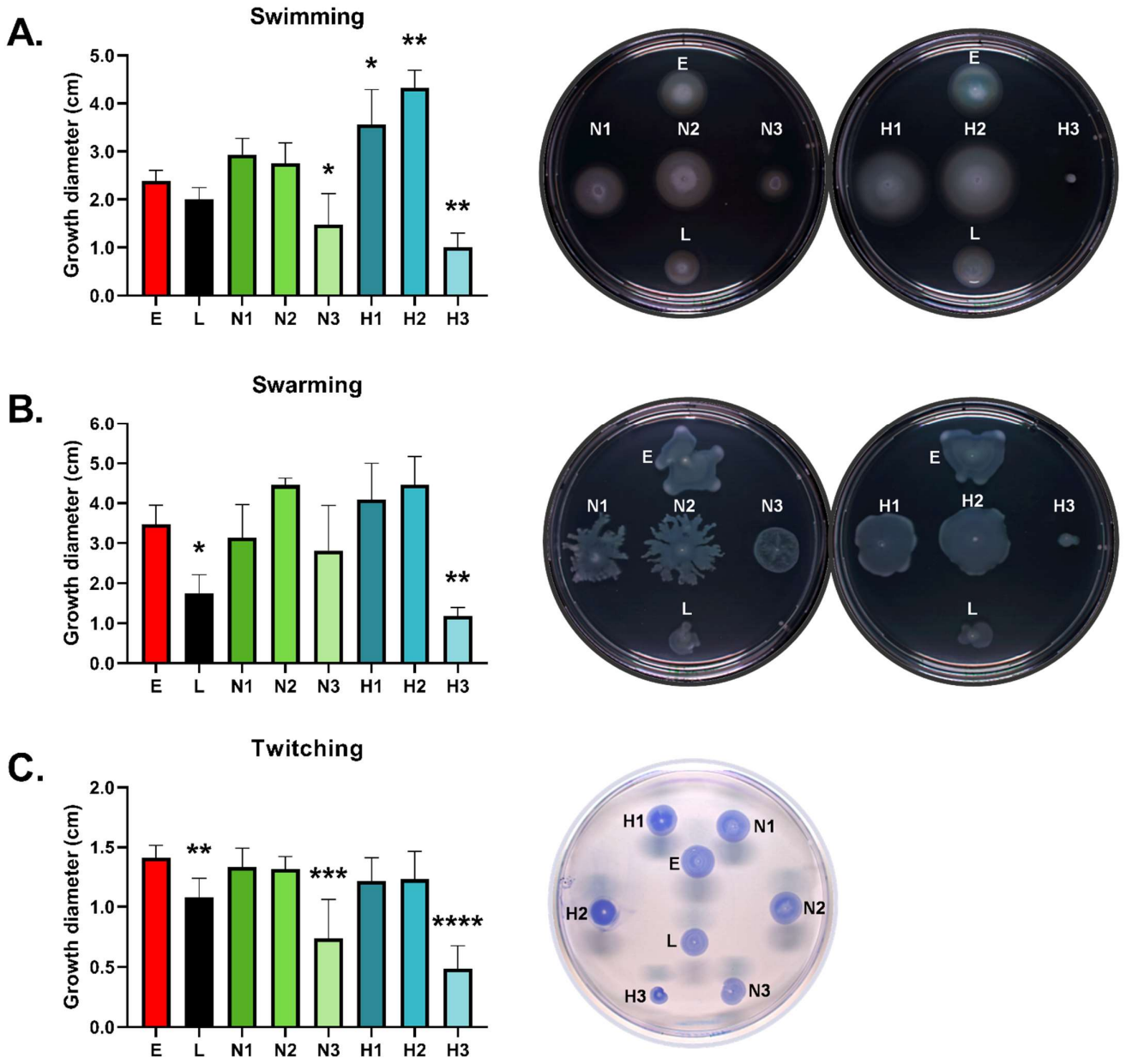

Figure 9. Effects of long-term hypoxia adaptation on *P. aeruginosa* motility. A. Changes in swimming motility**. B.** Changes in swarming motility. **C.** Changes in twitching motility. For each type of motility, a graph representing the average of diameter of the colony with bars representing data from at least 3 separate experiments with at least two technical replicates. Statistically significant difference by Kurskal-Wallis one-way ANOVA test compared to the early infection strain (E) with an uncorrected Dunn's test (*p< 0.05; **p< 0.01; ***p<0.001; ****p< 0.0001). E: early infection clinical isolate; L: late infection clinical isolate; N1, N2, N3: 28-day normoxia-adapted populations; H1, H2, H3: 28-day hypoxia adapted populations

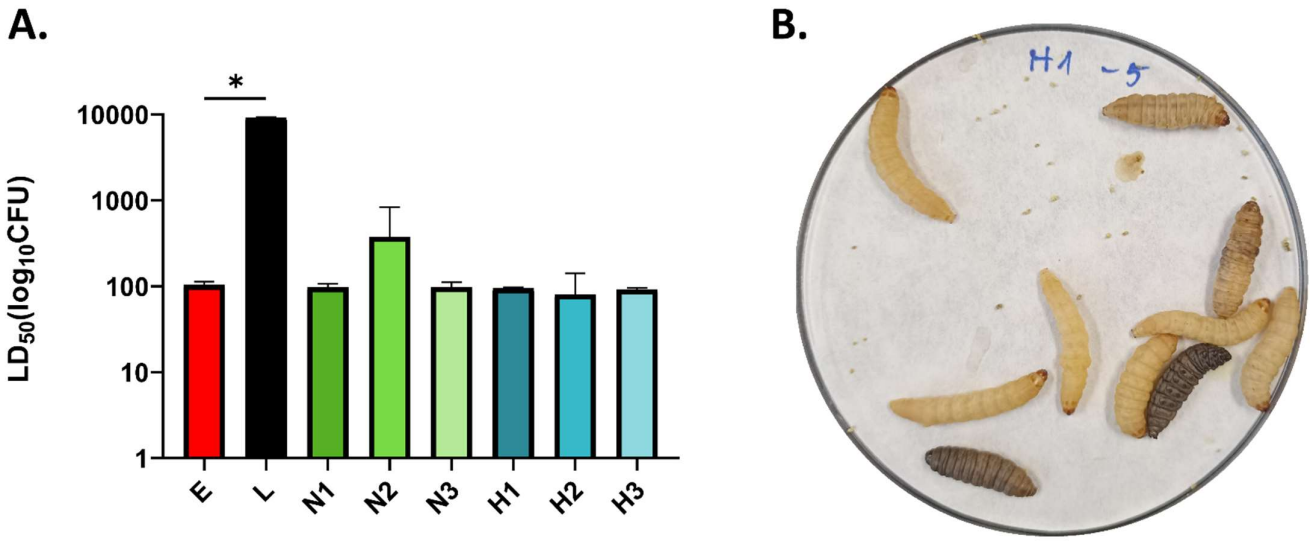

Fig. 10 Influence of long-term hypoxia on *P. aeruginosa* virulence in the *Galleria mellonela* model. A. Graph representing the average CFU needed to reach LD50 within 24h of the experiment from at least 3 separate repeats of the experiment**.** A touch to the larvae head was used to determine if they are alive. Statistically significant difference by Kurskal-Wallis one-way ANOVA test compared to the early infection strain (E) with an uncorrected Dunn's test is presented (*p< 0.05).). E: early infection clinical isolate; L: late infection clinical isolate; N1, N2, N3: 28-day normoxia-adapted populations; H1, H2, H3: 28-day hypoxia adapted populations. **B**. A representative picture showing the *G. mellonela* larvae melanisation. Healthy larvae with no disease symptoms are a bright cream colour. Larvae showing a slightly beige colour show first symptoms of infection, larvae with dark spots/stipes are clearly affected and the severely melanised larvae are in the late stages of the infection or dead.

A.

Phenotype		L	N1	N2	N3	H1	H2	H3
SCVs (%)		58.0%	0.00	0.00	2.7%	76.9%	79.8%	0.7%
Pyocyanin		↓	↓	=	=	↓	↓	=
Antibiotic resistance		=	=	=	=	↑	↑	=
Stress resistance	Osmotic	↓	↑	=	↑	↑	↑	↑
	Oxidative	=	=	=	↑	↑	↑	=
	Heat	↓	↓	↓	=	↓	↓	=
	Acidic	=	↑	↑	↑	=	=	=
Biofilm 72h		↑	=	↑	=	↑	↑	=
Motility	Swimming	↓	↑	↑	↓	↑	↑	↓
	Swarming	↓	=	↑	↓	↑	↑	↓
	Twitching	↓	=	↑	=	=	↑	↓
Siderophore production		↓	=	=	=	↓	↓	↓
Virulence (*Galleria mellonela*)		↑	=	=	=	=	=	=

B.

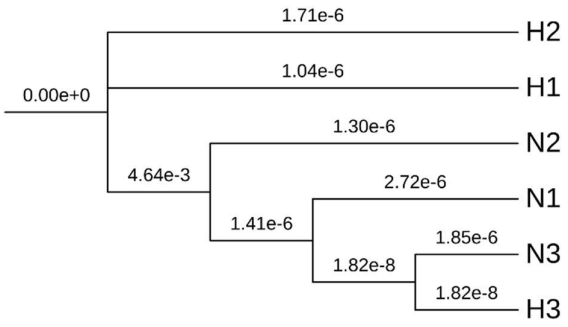

Fig. 11 Patterns of adaptation to long-term hypoxia. A. Summary of the phenotypic changes of adapted cultures. **B.** Phylogenetic tree of adapted *P. aeruginosa* populations generated by the iTOL Interacive tree of life (v6). The branch lengths are presented for each isolate.